Disease Models & Mechanisms 2, 247-266 (2009) doi:10.1242/dmm.000653

Inactivation of Drosophila Huntingtin affects long-term adult functioning and the pathogenesis of a Huntington's disease model

Sheng Zhang[1,5,*], Mel B. Feany[2], Sudipta Saraswati[4], J. Troy Littleton[4] and Norbert Perrimon[1,3,*]

SUMMARY

A polyglutamine expansion in the huntingtin (*HTT*) gene causes neurodegeneration in Huntington's disease (HD), but the in vivo function of the native protein (Htt) is largely unknown. Numerous biochemical and in vitro studies have suggested a role for Htt in neuronal development, synaptic function and axonal trafficking. To test these models, we generated a null mutant in the putative Drosophila *HTT* homolog (*htt*, hereafter referred to as *dhtt*) and, surprisingly, found that *dhtt* mutant animals are viable with no obvious developmental defects. Instead, *dhtt* is required for maintaining the mobility and long-term survival of adult animals, and for modulating axonal terminal complexity in the adult brain. Furthermore, removing endogenous *dhtt* significantly accelerates the neurodegenerative phenotype associated with a Drosophila model of polyglutamine Htt toxicity (HD-Q93), providing in vivo evidence that disrupting the normal function of Htt might contribute to HD pathogenesis.

INTRODUCTION

Huntington's disease (HD) is an autosomal dominant, progressive neurodegenerative disorder characterized clinically by deteriorating choreic movements, psychiatric disturbances and cognitive deficits (Gusella and MacDonald, 1995; Martin and Gusella, 1986; Vonsattel et al., 1985). HD is caused by an abnormal expansion of a polyglutamine (polyQ) tract at the N-terminus of a large cytoplasmic protein, huntingtin (Htt) (The Huntington's Disease Collaborative Research Group, 1993). The polyQ tract contains between 6 and 35 repeats in the wild-type Htt protein, whereas it is expanded to beyond 36 repeats in HD (The Huntington's Disease Collaborative Research Group, 1993). Numerous studies have demonstrated that mutant Htt containing an expanded polyQ tract is toxic to neurons (Cattaneo et al., 2001; Gusella and MacDonald, 2000). PolyQ expansion is also linked to at least eight other neurodegenerative disorders, collectively referred to as polyQ diseases (Riley and Orr, 2006; Zoghbi and Orr, 2000). Although Htt is ubiquitously expressed in the brain, HD mainly affects medium-sized spiny neurons in the striatum and to a lesser extent cortical pyramidal neurons that project to the striatum, suggesting that other cellular factors also contribute to pathogenesis (Cattaneo et al., 2001; Vonsattel and DiFiglia, 1998). Recent studies indicate that an alteration of wild-type Htt function might contribute to this specificity and to subsequent disease progression (Cattaneo et al., 2001). For example, mutant Htt can sequester wild-type Htt into insoluble aggregates, thereby exerting a dominant negative effect (Huang et al., 1998; Kazantsev et al., 1999; Narain et al., 1999; Preisinger et al., 1999; Wheeler et al., 2000). In addition, wild-type Htt can suppress the cell death induced by mutant polyQ-expanded Htt in vitro (Leavitt et al., 2001; Van Raamsdonk et al., 2005). Furthermore, wild-type Htt is proposed to have a neuroprotective role as expression of Htt can protect cultured striatal neurons from stress- and toxin-mediated cell death (Rigamonti et al., 2000).

Since its identification, the normal function of Htt has been subject to extensive investigation (Cattaneo et al., 2001; Harjes and Wanker, 2003). The murine Htt homolog (also known as Hdh) is essential during early mouse development, as *Htt*-null mice die during gastrulation at embryonic day 7.5 (Duyao et al., 1995; Nasir et al., 1995; Zeitlin et al., 1995). Chimeric analysis demonstrated that the early embryonic lethality is the result of a crucial role of Hdh in extraembryonic membranes, as this lethality can be rescued by providing wild-type Hdh function in extraembryonic tissue (Dragatsis et al., 1998). Conditional knockout of Hdh in the mouse forebrain at postnatal or late embryonic stages causes a progressive neurodegenerative phenotype, lending support to the hypothesis that depletion of normal Htt activity during disease progression contributes to HD pathogenesis (Dragatsis et al., 2000). A more recent study in zebrafish, which used morpholino oligos to transiently knockdown endogenous Htt, suggests that Htt has a role in normal blood function and iron utilization (Lumsden et al., 2007). Currently, little is known about the normal biological function of wild-type Htt (Cattaneo et al., 2005).

Htt encodes a large cytoplasmic protein of 350 kDa. Structural analysis of Htt proteins identified the presence of many HEAT (huntingtin, elongation factor 3, the A subunit of protein phosphatase 2A and TOR1) repeats, which are approximately 40-amino acid (a.a.) long structural motifs, composed of two anti-parallel helices, of unknown function (Andrade and Bork, 1995). No other domains have been identified in Htt to suggest a biological function for the protein. Functional studies in mammalian systems, mainly from protein interaction assays, have associated Htt with diverse cellular processes including: endocytosis; modulation of

[1]Department of Genetics, [2]Department of Pathology and [3]Howard Hughes Medical Institute, Brigham and Women's Hospital, 77 Avenue Louis Pasteur, Harvard Medical School, Boston, MA 02115, USA
[4]The Picower Institute for Learning and Memory, Department of Biology and Department of Brain and Cognitive Sciences, Massachusetts Institute of Technology, Cambridge, MA 02139, USA
[5]Present address: Research Center for Neurodegenerative Diseases, The Brown Foundation Institute of Molecular Medicine, University of Texas Health Science Center at Houston, 1825 Pressler Street, Houston, TX 77030, USA
*Authors for correspondence (e-mail: szhang@genetics.med.harvard.edu; perrimon@receptor.med.harvard.edu)

synapse structure and synaptic transmission; transcriptional regulation, especially of the brain-derived neurotrophic factor (BDNF) which is essential for the survival of the striatal neurons affected in HD; axonal transport of BDNF and vesicles; and apoptosis (Cattaneo et al., 2001; Cattaneo et al., 2005; Harjes and Wanker, 2003; Zuccato et al., 2001; Zuccato and Cattaneo, 2007). Importantly, only a few of these proposed functions of Htt have been directly tested in vivo owing to the early embryonic lethality associated with *Htt*-null mutant mice.

In an extensive search for Htt homologs in other species, Li et al. (Li et al., 1999) identified a single *HTT* homolog in Drosophila (*htt*, hereafter referred to as *dhtt*). By sequence comparison, the homologous regions between Drosophila and human Htt proteins are mainly located within five discrete areas, including three relatively large continuous regions and two small segments, that cover about one-third of the total protein length (supplementary material Fig. S1A). At the amino acid level, these homologous regions, which are comprised of about 1200 a.a. residues in Drosophila Htt (dHtt), share around 24% identity and 49% similarity (Li et al., 1999). In addition to the sequence similarity, other shared features support the proposal that the Drosophila gene identified in the study by Li et al. is indeed the fly homolog of human Htt (Li et al., 1999). For example, in terms of the protein size, both the Drosophila and human Htt proteins are unusually large and contain 3583 and 3144 a.a. residues, respectively (Li et al., 1999). In addition, the regions with a relatively high level of conservation are not only clustered in large continuous stretches, but are also located in the same order and distributed over the entire length of the proteins. Moreover, *dhtt* and mammalian HD genes share similar patterns of gene expression (Li et al., 1999) (Fig. 1). Interestingly, although an *HTT* homolog exists in Drosophila, no *HTT*-like gene has been found in other less complex eukaryote species such as *C. elegans* or the yeast *S. cerevisiae* (Li et al., 1999).

The identification of a Drosophila Htt homolog provides a unique opportunity to evaluate the role of Htt in this well-established genetic model system. Several cellular processes implicated in Htt function, including axonal transport and synapse formation, have been well-characterized in Drosophila, allowing an in vivo evaluation of their relationship with Htt. Further, as fly models of HD have been well-established, this model allows an in vivo examination of the function of endogenous Htt in HD pathogenesis (Marsh and Thompson, 2006; Steffan et al., 2001). In this study, we report the isolation of a *dhtt* mutant and describe its phenotype. Further, we examine how the removal of endogenous *dhtt* affects several cellular processes that have previously been implicated with Htt, and test how the loss of endogenous *dhtt* affects the pathogenesis associated with an established Drosophila model of polyQ toxicity (HD-Q93).

RESULTS

HEAT repeats in dHtt

Considering the limited sequence homology between mammalian and fly Htt, it is important to examine the extent of the structural similarity between these proteins. In the Htt family proteins, the HEAT repeat is the only identifiable structural motif (Andrade and Bork, 1995; Cattaneo et al., 2005). A previous phylogenetic study identified 16 HEAT repeats in human Htt and, notably, 14 of these 16 repeats were also found in insect Htt proteins including dHtt (Tartari et al., 2008). A less stringent structural analysis predicted up to 40 HEAT repeats (including the AAA, ADB and IMB subgroups) in human Htt (see Methods). Interestingly, using the same parameter, 38 HEAT repeats could be identified in dHtt (see supplementary material Fig. S1 for details of the predicted HEAT repeats). Further, these HEAT repeats span the entire length of each protein and have a similar distribution, clustering in four groups at the N-, middle- and C-terminal regions, which have a large overlap with their segments of homologous sequences (supplementary material Fig. S1B). Although further studies are needed to elucidate the structure of the Htt proteins, this rather remarkable similarity raises the possibility of a conserved secondary structure among Htt family proteins and that both human and Drosophila Htt proteins are composed largely of repeated HEAT motifs.

Ubiquitous expression of *dhtt* in Drosophila

Previous analysis has shown that *dhtt* is widely expressed during all developmental stages from embryos to adults (Li et al., 1999). We confirmed the expression of the *dhtt* transcript in adults using reverse transcription (RT)-PCR (data not shown) (Fig. 5C). To examine the tissue-specific *dhtt* expression, we performed whole-mount RNA in situ hybridization. Staining with two DIG-labeled antisense probes, targeting different regions of *dhtt*, revealed similar ubiquitous *dhtt* expression at different stages of fly embryogenesis and in larval tissues (Fig. 1A-F and data not shown), whereas a positive control performed in parallel gave rise to robust in situ signals (supplementary material Fig. S2). Importantly, of the two negative controls included in the assay, one using sense *dhtt* RNA probes on wild-type samples (Fig. 1B) and the other using the same set of antisense *dhtt* RNA probes against tissues from a *dhtt* deletion mutant that had been generated subsequently (Fig. 1F), both produced much weaker background signals. Together, these data indicate that *dhtt* is widely expressed at low levels during all stages of Drosophila development.

dHtt is a cytoplasmic protein

Mammalian Htt proteins are largely cytoplasmic with a widespread expression pattern (DiFiglia et al., 1995; Gutekunst et al., 1995; Sharp et al., 1995). To determine the expression and subcellular localization of the endogenous dHtt protein, we developed an affinity-purified polyclonal antibody against dHtt. The specificity of this antibody was confirmed by its ability to recognize ectopically expressed dHtt protein in transfected Drosophila S2 cells (Fig. 1G,H) and larval tissues (Fig. 1I-K). When the dHtt protein was ectopically expressed from a UAS-*dhtt* transgene by using a *patched*-Gal4 driver, our anti-dHtt antibody could easily detect the striped pattern of dHtt expression in the middle of imaginal discs, which is the characteristic domain of Patched expression (Fig. 1I). In wild-type animals, use of the anti-dHtt antibody resulted in low-level ubiquitous staining in embryos, larval and adult tissues, with no specific pattern of protein expression (data not shown). At the subcellular level, ectopically expressed dHtt was found predominantly in the cytoplasm in transfected S2 cells and in larval tissues (Fig. 1G-K and data not shown), suggesting that dHtt, similar to its human counterpart, is mainly a cytoplasmic protein.

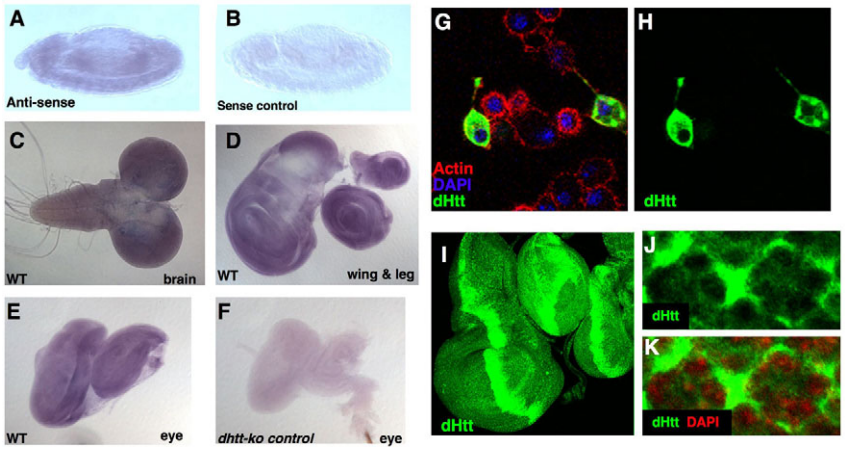

Fig. 1. Ubiquitous expression of *dhtt* in Drosophila. (A-F) *dhtt* is widely expressed at a low level during Drosophila development, as revealed by whole-mount in situ hybridization. (A,B) Stage 15 Drosophila embryos stained with digoxigenin (DIG)-labeled *dhtt* antisense probes revealed the low-level and ubiquitous expression of the *dhtt* transcript (A); control embryos at the corresponding stage, which were stained with *dhtt* sense probes, showed only minimal background signals (B). All embryos are lateral views, anterior to the left and dorsal side up. (C-F) Third instar larval tissues hybridized with *dhtt* antisense probes. Low-level and ubiquitous *dhtt* expression was observed in the brain (C), wing and leg (D) and eye imaginal discs (E). (F) A negative in situ control – an eye imaginal disc from a *dhtt* deletion mutant stained in parallel – showed only minimal background signals. (G-K) The dHtt protein predominantly localizes to the cytoplasm. (G,H) In transfected Drosophila S2 cells, ectopically expressed dHtt protein (green) was found predominantly in the cytoplasm; it was also found on cellular protrusions, but was mostly excluded from the nucleus. (G) Overlaying images of the S2 cells co-stained with phalloidin (red), which detects F-actin, and the DNA dye DAPI (blue) reveal the overall cell morphology and the cell nuclei, respectively. (I-K) Cytoplasmic localization of the dHtt protein (green) ectopically expressed in Drosophila third instar larval imaginal disc tissues. (I) The anti-dHtt antibody can recognize overexpressed dHtt in the *patched* expression domain driven by *patched*-Gal4 and shows the characteristic striped dHtt expression pattern in the middle of the wing and leg imaginal discs. Genotype: *patched*-Gal4/+>UAS-*dhtt*/+. (J,K) High-magnification view of an eye imaginal disc with ectopically expressed dHtt protein [green (J)], which shows a mainly cytoplasmic localization. (K) Overlaying images of the same eye disc region co-stained with DAPI (red) to reveal the cell nuclei. Genotype: GMR-Gal4/+>UAS-*dhtt*/+.

Creating a *dhtt* deletion

Similar to human Htt, *dhtt* encodes an unusually large protein of 3583 a.a. residues. The cDNA for the *dhtt* gene is 11,579 base pairs (bp) long and is derived from 29 exons in a 38 kb transcribed genomic region at cytological interval 98E2 (Li et al., 1999) (Fig. 2A,C). No null mutations in *dhtt* have been isolated previously. To generate a null mutant for dHtt, we selected two FRT-bearing insertion lines surrounding *dhtt*: p-element d08071, which is inserted at the 5′ end of the neighboring *CG9990* gene, and piggyBac insertion f05417, which is located inside the intron between *dhtt* exon 27 and exon 28 near the 3′ end of the gene (Fig. 2A). Using flipase (FLP)–FRT-mediated recombination (Parks et al., 2004), we generated a precise deletion of 55 kb between the two insertions (see Methods). This deletion allele, termed *Df(98E2)*, removed most of the *CG9990* gene and 34 kb of the 38 kb genomic-coding region for *dhtt*, with only the last two exons of the *dhtt* gene remaining (Fig. 2A-C). The deletion was confirmed by inverse PCR from extracted genomic DNA and by DNA sequencing (data not shown).

Drosophila containing the *Df(98E2)* deletion, which removes both *CG9990* and *dhtt*, are homozygous lethal at the embryonic stage. *CG9990* encodes a previously uncharacterized protein belonging to the ABC transporter superfamily (Dean et al., 2001). To separate the mutant phenotype of *dhtt* from *CG9990*, we generated transgenic flies carrying a *CG9990* genomic rescue transgene in the *Df(98E2)* background (see Methods). These lines, referred to as *dhtt-ko* (*dhtt*-knockout only), carry both the *CG9990* rescue transgene and the *Df(98E2)* deletion, and thus are mutant only for *dhtt* (Fig. 2B-D).

dhtt is dispensable for Drosophila development

The *dhtt-ko* allele removes 27 of the 29 exons of *dhtt* (Fig. 2). Since *Htt* homozygous knockout mice die during early embryogenesis (Duyao et al., 1995; Nasir et al., 1995; Zeitlin et al., 1995), we expected that loss of *dhtt* in the fly would be associated with prominent developmental defects. However, *dhtt-ko* flies are homozygous viable, demonstrating that the lethality observed following the *Df(98E2)* deletion is caused by loss of *CG9990*. To verify that the *dhtt* gene is indeed deleted in *dhtt-ko* flies, we extracted genomic DNA from homozygous *dhtt-ko* adults and performed a Southern blot analysis. As shown in Fig. 2D, all genomic DNA containing the *dhtt* gene was removed in *dhtt-ko* flies except for the final two 3′ exons.

Further analyses demonstrated that homozygous *dhtt-ko* flies develop at a similar rate to wild-type flies and give rise to fertile adults with no discernible morphological abnormalities. The progeny derived from homozygous *dhtt-ko* flies did not show a reduction in viability or display other obvious developmental defects, suggesting that maternally contributed *dhtt* has no significant effect on animal development or function.

To determine whether developmental defects are present in *dhtt-ko* animals, we characterized *dhtt-ko* mutants using a variety of cellular and neuronal markers. These studies failed to reveal any obvious developmental abnormalities during embryogenesis, or during larval and adult stages (Fig. 3 and data not shown). In particular, the embryonic central nervous system (CNS) (Fig. 3A) and muscles, and the larval muscles, CNS, eye and other imaginal discs all appeared normal (Fig. 3B and data not shown). Further,

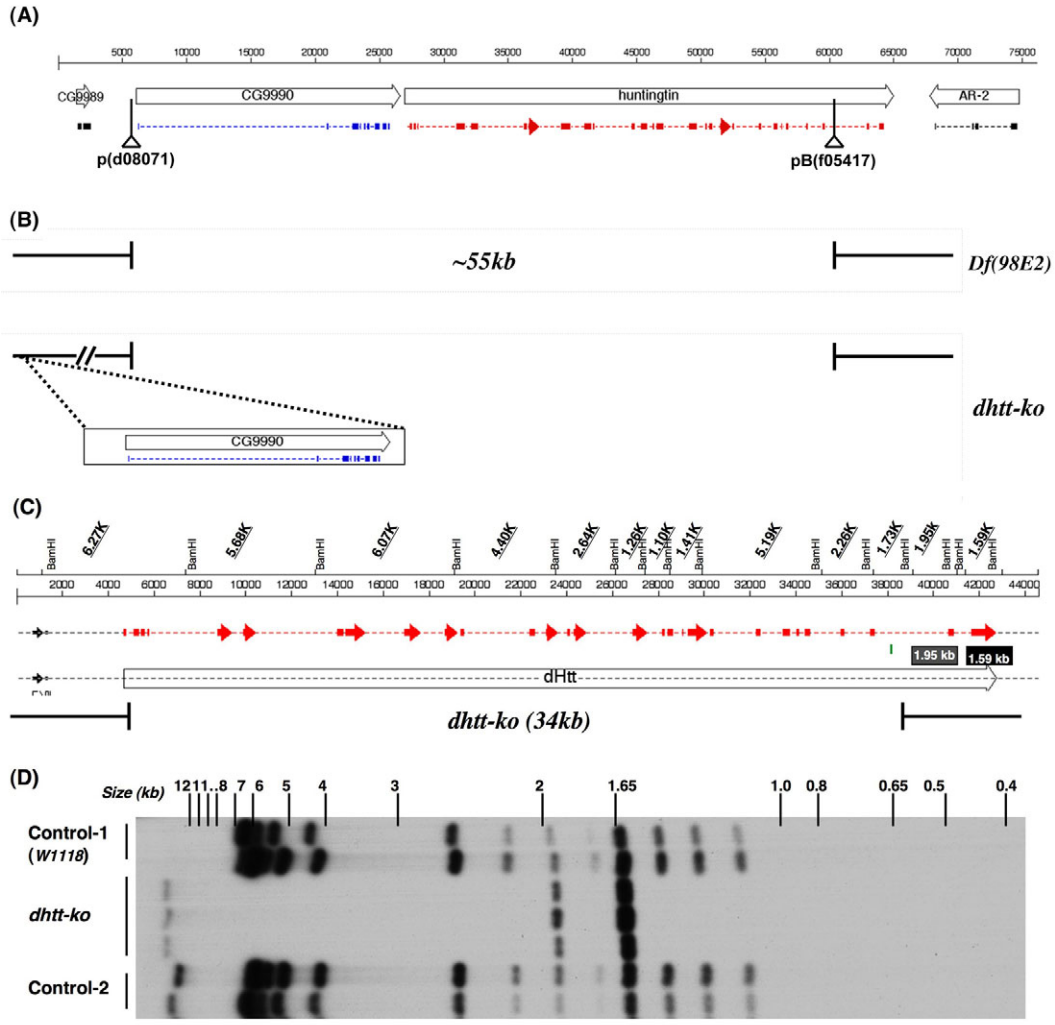

Fig. 2. Genomic organization of the *dhtt* locus and the *dhtt-ko* deletion. (A) The genomic structure of cytological region 98E2. The scale bar on top indicates the gene size (in base pairs). The position and transcriptional direction of *dhtt* and nearby genes (open boxes) is shown; introns (dashed lines) and exons (colored filled boxes) are labeled, as well as the FRT insertions (triangles) used for generating the *Df(98E2)* deficiency. (B) *dhtt-ko* was generated by an FRT-mediated precise deletion [*Df(98E2)*] of a 55 kb genomic region covering most of *CG9990* and *dhtt*. A genomic transgene covering the entirety of *CG9990* (open box) was reintroduced as a transgenic construct in the *Df(98E2)* background. (C) Detailed genomic structure of the *dhtt* gene. The scale bar, with predicted *Bam*HI fragments, is drawn at the top. The exons of the *dhtt* gene are depicted as red arrows and squares, whereas introns are highlighted as red dashed lines, both are drawn to scale. (D) The *dhtt-ko* removes all but the last two of the 29 exons in *dhtt*, as verified by Southern blotting using *Bam*HI digestion of genomic DNA. DNA extracted from control and *dhtt-ko* adult animals was hybridized with a DNA probe targeting all exons of *dhtt* (see Methods). The two *Bam*HI fragments (1.95 kb and 1.59 kb) that contain the last two remaining exons in *dhtt-ko* mutants are highlighted in (C).

in aged adults (40-day-old flies), the external eye morphology was normal and the eight neuronal photoreceptor cells in each ommatidium were clearly present, together with their accessory cells (Fig. 3C,D). We note that our finding is different from a recent study that examined *dhtt* function using RNA interference (RNAi), which implicated a role for *dhtt* in axonal transport and eye integrity (Gunawardena et al., 2003). The exact nature of this phenotype discrepancy is not clear. Given the experiment was carried out at 29°C, it is possible that the observed RNAi phenotypes were the result of cellular toxicity caused by the high-level expression of Gal4 (Gunawardena et al., 2003). The more severe phenotypes might also be the result of the non-specific RNAi off-target effects caused by the knockdown of unrelated genes (Kulkarni et al., 2006). Nevertheless, our results suggest that *dhtt* is dispensable for normal Drosophila development. This result is in contrast to the essential role of *Htt* in mouse (Duyao et al., 1995; Nasir et al., 1995; Zeitlin et al., 1995). These phenotypic differences are probably the result of differences in mouse and fly embryogenesis, as the early lethality of *Htt*-null mice is due to the function of Hdh in extraembryonic membranes, for which there are no equivalents in Drosophila (Dragatsis et al., 1998) (see Discussion).

Normal synapse organization in *dhtt-ko*

Htt has been reported to interact with a diverse group of proteins whose functions have been directly or indirectly linked to synapse organization and synaptic activity (Harjes and Wanker, 2003),

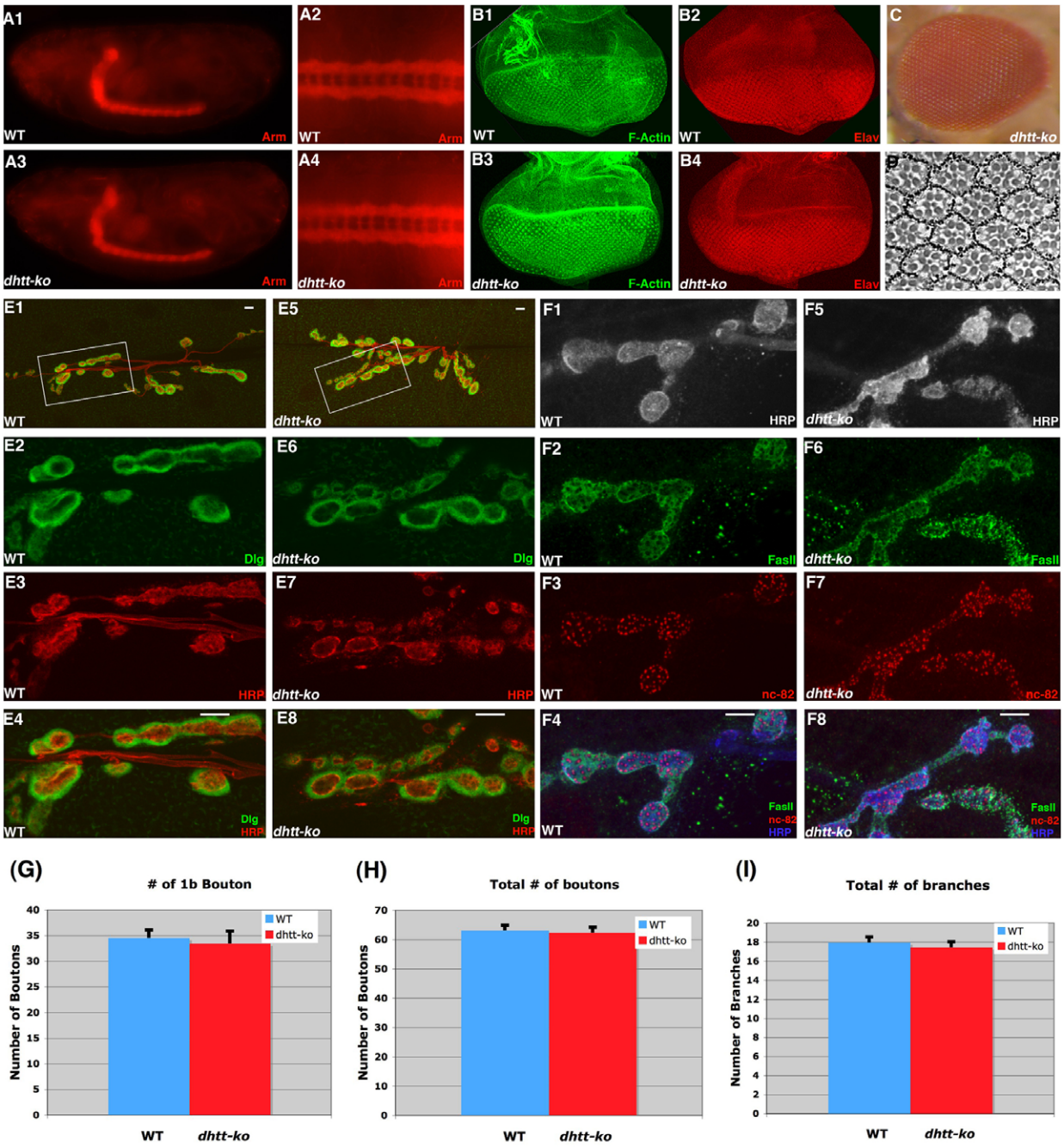

Fig. 3. *dhtt* is dispensable for Drosophila development. (A) Normal development of the CNS during embryogenesis in *dhtt-ko* flies (A3,A4) compared with wild-type controls (A1,A2), as revealed by anti-Armadillo staining. (A2,A4) Enlarged views of the ventral nerve cord in wild-type (A2) and *dhtt-ko* (A4) embryos show its regular ladder-like structure. (B) Differentiation and patterning of the eye during the third instar larval stage in *dhtt-ko* flies (B3,B4) is indistinguishable from wild-type controls (B1,B2), as revealed by anti-Elav staining (red) (B2,B4) to label differentiated neurons and phalloidin staining for F-actin (green) (B1,B3) to reveal the overall cytoskeleton organization. (C,D) Eye images of 40-day-old *dhtt-ko* mutants. Both the overall external eye morphology (C) and the internal organization of neuronal photoreceptors (D) are normal, even in the 40-day-old *dhtt-ko* adults. (E-I) Synaptic development is normal in *dhtt* mutants. Low (E1,E5) and high (E2-E4,E6-E8,F1-F8) magnification confocal images of glutamatergic NMJs in the abdominal segment A3 of third instar muscles 6 and 7. (E) NMJs are double-labeled with the neuronal membrane marker anti-HRP (red) and anti-Dlg (green), which reveal the well-defined presynaptic and postsynaptic NMJ structures in wild-type (E1-E4) and *dhtt-ko* mutants (E5-E8). (E2-E4,E6-E8) Magnified views of the areas highlighted in (E1,E5). (F) NMJs are labeled with anti-HRP (white) (F1,F5), the periactive zone marker anti-FasII (green) (F2,F6) and the active zone marker nc82 (red) (F3,F7), revealing the normal periactive zone and active zone organization in wild-type (F1-F4) and *dhtt-ko* flies (F5-F8). (F4,F8) Overlayed images of (F1-F3,F5-F7), respectively. WT: w^{1118} wild-type control. Bar, 5 µm (in all panels). (G-I) Quantitative analysis of NMJs in muscle 6 and 7 of the abdominal segment A3 for wild-type control (WT, blue) and *dhtt-ko* mutant (red) flies. (G) Average number of type 1b boutons: WT control=34.5±1.6 (*n*=24), *dhtt-ko* mutants=33.5±2.4 (*n*=21); the difference is statistically insignificant, *P*=0.72 (Student's *t*-test). (H) Average number of total boutons: WT control=63.1±1.8 (*n*=24), *dhtt-ko* mutants=62.3±2.0 (*n*=21); *P*=0.76. (I) Total number of branches: WT control=18.0±0.6 (*n*=28), *dhtt-ko* mutants=17.4±0.6 (*n*=34); *P*=0.52. The data in (G-I) are presented as the means±s.e.m. (standard error of the mean).

including proteins that regulate cytoskeleton dynamics and clathrin-mediated endocytosis [e.g. HIP1 (Sla2p), HIP12, PACSIN/syndapin 1 and endophilin 3] (Chopra et al., 2000; Higgins and McMahon, 2002; Kalchman et al., 1997; Modregger et al., 2002; Seki et al., 1998; Singaraja et al., 2002; Sittler et al., 1998; Wanker et al., 1997); axonal vesicle transport (e.g. HAP1) (Engelender et al., 1997; Gunawardena et al., 2003); and dendritic morphogenesis and synaptic plasticity (e.g. the postsynaptic density protein DLG4/PSD95 and the adaptor proteins GRB2 and TRIP10/CIP4) (Holbert et al., 2003; Liu et al., 1997; Sun et al., 2001). To test whether *dhtt* plays a role in synapse organization, we examined the formation of glutamatergic neuromuscular junctions (NMJs) in third instar larvae, a well-characterized system for studying synapse formation and function in Drosophila (Budnik and Gramates, 1999). Examination with a panel of synapse markers showed that axonal pathfinding, muscle innervation and overall synapse structure are normal in *dhtt* mutants (Fig. 3 and data not shown). Double-labeling with the axonal membrane marker anti-HRP and the postsynaptic density marker anti-Dlg (the Drosophila PSD95 homolog) revealed well-organized presynaptic and postsynaptic structures (Fig. 3E1-E8), as well as an enrichment of synaptic vesicles at the synapses, with no obvious synapse retraction phenotype (data not shown). Moreover, *dhtt* mutants showed normal organization of the presynaptic microtubule (MT) cytoskeleton, with the presence of stable MT bundles traversing the center of NMJ branches and a dynamically reorganized MT network at distal boutons (data not shown). Quantification of NMJ bouton number and axonal branching did not reveal a significant difference between wild-type controls and *dhtt* mutants (Fig. 3G-I). Finally, *dhtt* mutants displayed the stereotypical complementary pattern of active zones surrounded by the honeycomb-like organization of periactive zones, and examination of multiple synaptic proteins such as nc82 (an active zone marker) and fasciclin II (FasII, a periactive zones marker) showed normal synaptic localization (Fig. 3F1-F8). As a control, we also examined synapse organization in *CG9990* transgenic animals, which displayed similar well-organized NMJ structures (supplementary material Fig. S3 and data not shown). Together, these results suggest that *dhtt* is not essential for synapse formation and organization at NMJs.

dhtt is not essential for axonal transport

Htt has also been proposed to regulate axonal vesicle transport because one of its binding partners, HAP1, interacts directly with p150Glued, which is an essential subunit of the dynactin complex involved in regulating dynein-mediated retrograde axonal transport (Engelender et al., 1997; Gunawardena et al., 2003; Harjes and Wanker, 2003). In Drosophila, individuals that are defective for essential components of the axonal transport machinery often display characteristic mobility phenotypes, such as tail flipping during larva crawling, and progressive lethargy and paralysis (Gindhart et al., 1998; Gunawardena and Goldstein, 2001; Martin et al., 1999). Such mutant animals also develop an axonal swelling phenotype, owing to the abnormal accumulation of synaptic vesicles along axons, and fail to properly deliver and localize synaptic components to the termini (Gindhart et al., 1998; Gunawardena and Goldstein, 2001; Martin et al., 1999). *dhtt* mutants showed normal crawling behavior during larval stages. Furthermore, the distributions of the synaptic vesicle markers anti-synaptotagmin (Syt) and anti-cysteine string protein (CSP) were normal, revealing no obvious accumulation or axonal swellings (Fig. 4 and data not shown). Further, immunostaining with other synaptic components, including synapsin (a reserved vesicle pool marker), FasII (a periactive zone marker) and Dlg, demonstrated that synaptic components were properly delivered to synapses (Fig. 3E-F and data not shown). Similarly, examination of *CG9990* transgenic animals failed to reveal discernible larval mobility or axonal transport defects (supplementary material Fig. S3). Together, these results suggest that *dhtt* does not play an essential role in axonal transport.

dhtt is crucial for aged adults

We next investigated whether *dhtt* might function in adult animals. We examined whether newly emerged *dhtt* adults were hypersensitive to stress tests including prolonged heat and cold exposure, vortexing and feeding with the oxidative stress compound paraquat. In these tests, *dhtt* mutants showed similar responses to wild-type controls (data not shown). Thus, unlike flies that are mutated for Parkinson's disease genes such as *parkin* and *pink1*, which are sensitive to multiple stress challenges (Clark et al., 2006; Greene et al., 2003; Park et al., 2006), loss of *dhtt* does not render young adult animals more vulnerable to environmental stresses.

Next, we followed the activity and viability of *dhtt* animals throughout the adult life cycle. Although no discernible difference in the activity and survival rate was observed between *dhtt-ko* and wild-type young adults, we observed striking defects in older adult *dhtt-ko* flies. *dhtt-ko* animals showed similar spontaneous locomotion to that of wild-type controls at day 15 and earlier (Fig. 5A; supplementary material Movie 1). However, as flies aged, *dhtt-ko* mutants displayed a rapidly declining mobility, which was evident by day 25. By day 40, almost all *dhtt* mutants showed severely compromised mobility (Fig. 5A; supplementary material Movie 2) and their viability declined quickly. Whereas, on average, half of the wild-type controls died around day 59 but could live for up to 90 days, half of the *dhtt-ko* flies died around day 43 and almost all by day 50 (Fig. 5B).

To verify that the late-onset mobility and viability defects were because of loss of *dhtt*, we constructed a *dhtt* minigene that expressed full-length *dhtt* under the control of its endogenous regulatory region (see Methods). In the presence of this mini-*dhtt* transgene, the expression of the *dhtt* gene was restored in *dhtt-ko* mutants, as confirmed by RT-PCR (Fig. 5C) Both the late-onset mobility and viability phenotypes observed in *dhtt-ko* mutants were rescued by the *dhtt* transgene (Fig. 5A,B; supplementary material Movie 3). Importantly, introduction of an unrelated transgene construct, such as *elav*-Gal4 (Fig. 5B) or UAS-eGFP (data not shown), into the *dhtt-ko* background could not rescue the mobility and viability phenotypes of *dhtt-ko* mutants, confirming that the rescue was because of the restored expression of *dhtt*. Thus, although *dhtt* is not essential for normal Drosophila development, its function is important in maintaining the long-term mobility and survival of adult animals.

dhtt-ko is dispensable for normal neurotransmission

The observed mobility and viability phenotype could be because of an underlying neurotransmission defect in *dhtt* mutants as several proposed Htt functions, such as axonal vesicle transport

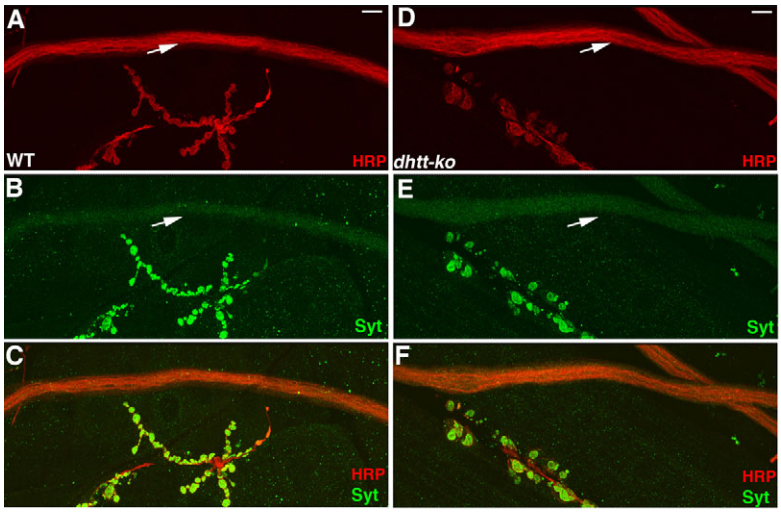

Fig. 4. Normal axonal transport in *dhtt-ko* mutants. Confocal images of wild-type control (A-C) and *dhtt-ko* (D-F) NMJs and neighboring axons (white arrows) of the larval peripheral nervous system (anti-HRP, red). Synaptic vesicles (green, anti-Syt) are properly delivered to NMJs and show no obvious accumulation in the axons of *dhtt-ko* mutants (D-F), similar to the wild-type controls (A-C). Signals for Syt were overexposed in (B,C,E,F) in order to reveal any possible abnormal accumulations of synaptic vesicles within axons (white arrows). (C,F) Overlayed images of double staining with anti-HRP and anti-Syt. WT: w^{1118} wild-type control. Bars, 10 μm.

and clathrin-mediated endocytosis in neurons, are essential for the delivery and recycling of synaptic vesicles at nerve terminals to ensure effective neurotransmission (Cattaneo et al., 2001; Eaton et al., 2002; Harjes and Wanker, 2003; Hinshaw, 2000; Slepnev and De Camilli, 2000). To test the neuronal communication in *dhtt* mutants, we measured synaptic physiology at the well-characterized third instar larval NMJ. We quantified the amplitude of evoked excitatory junctional potentials (EJPs), resting membrane potential and paired-pulse facilitation (PPF) (Fig. 6A-D and data not shown). In adult animals, we recorded electroretinogram (ERG) responses in the eye and quantified DLM (dorsal longitudinal flight muscle) bursting activity in the giant fiber flight circuit (Fig. 6E and data not shown). Following exhaustive analysis, we found no significant defect in either synaptic transmission or short-term plasticity in *dhtt* mutants. Together, these data suggest that *dhtt* is not essential for neurotransmission.

To investigate whether the observed mobility and viability phenotypes in aged *dhtt* mutants are correlated with neuronal communication defects, we screened for electrophysiological phenotypes in animals aged 40-45 days, when behavioral motor abnormalities are prominent. Aged *dhtt* mutant adults did not display abnormal seizure activity in extracellular recordings from DLM flight muscles in the giant fiber escape pathway, as has been observed in temperature-sensitive Drosophila mutants that have altered synaptic transmission (Guan et al., 2005). Aged mutants also showed normal visual transduction and synaptic transmission in the visual system at room temperature (Fig. 6E and data not shown), consistent with the observation that *dhtt* does not play a crucial role in neurotransmission.

Previous studies have shown that mutations affecting synaptic function often manifest a more prominent phenotype under temperature-induced stress (Atkinson et al., 1991; Coyle et al., 2004). To assess whether phototransduction can be maintained under an elevated temperature in *dhtt* mutants, we performed ERG recordings at 37°C. Although *dhtt* mutants aged 1-3 days displayed normal ERGs at both 20°C and 37°C, aged *dhtt* mutants displayed abnormal sensitivity to 37°C, with over 60% of aged mutants losing light-induced phototransduction and the on/off transients at 37°C compared with only 20% of control aged adults (Fig. 6E,F), indicating an important role of *dhtt* in maintaining phototransduction under temperature-induced stress. Given that aged *dhtt* mutant adults did not show additional motor defects when placed at 37°C, we hypothesize that the loss of photoreceptor depolarization found in ERG recordings reflects temperature-sensitive defects in the phototransduction cycle, rather than in synaptic transmission. These results suggest that aged *dhtt* mutants are more sensitive to stress than young *dhtt* animals or aged controls.

Reduced axon terminal complexity in *dhtt-ko* brains

To further test for *dhtt* function in the adult brain, we examined *dhtt* brain morphology using a series of cellular markers. The overall patterning and gross morphology of *dhtt-ko* brains appeared normal, as shown by staining with antibodies such as the glial cell marker anti-Repo, the pan-neuronal marker anti-Elav and the synaptic vesicle marker anti-CSP (data not shown). In addition, within the ventral nerve cord, the neuropile was similarly enriched with synaptic vesicles. Further, the overall axonal morphology of *dhtt-ko* mutants appeared normal with no clear axonal blebbing or defasciculation phenotypes (data not shown). Interestingly, examination of the mushroom bodies (MBs), which are involved in learning and memory in flies, by anti-FasII staining revealed that the signal intensity was weaker in *dhtt* mutants than in wild-type controls, despite appearing morphologically normal (Fig. 7J,M). Quantification of MB size and FasII staining signals revealed that, although there was a slight reduction in the average size of MBs in *dhtt-ko* mutants compared with wild-type controls (Fig. 7P) (average area covered by each MB: wild type=13,352±156 μm^2, *dhtt-ko* mutant=11,927±310 μm^2; P=0.0003), the average signal intensity of FasII signals in the MBs of *dhtt-ko* mutants was decreased by ~50% (Fig. 7Q) (relative signal intensity of MBs: wild type=100±5.8/μm^2, *dhtt-ko* mutant=47.7±6.1/μm^2; P<0.0001; total number of MBs quantified: wild-type control, n=13; *dhtt-ko* mutants, n=10).

To examine the effect of *dhtt* loss-of-function on the detailed structure of individual neurons in the brain, we used the A307-Gal4 line, which labels the pair of giant fiber (GF) neurons and a small number of other neurons of unknown identity in the adult brain, to examine axonal projection patterns and the fine axonal terminal structure of individual neurons (Phelan et al., 1996) (Fig.

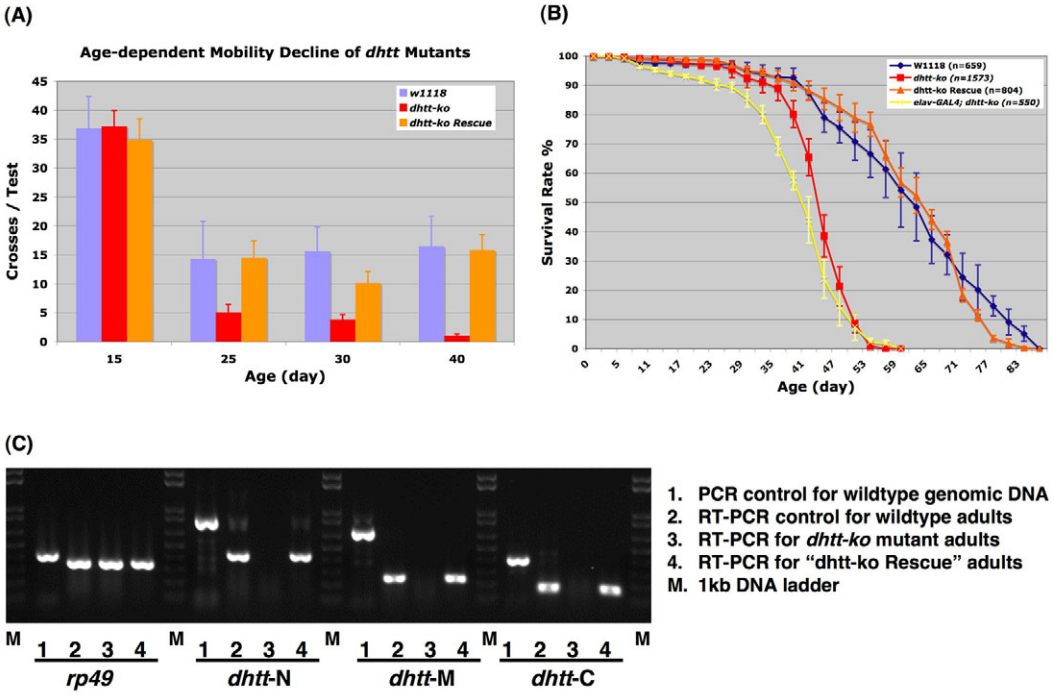

Fig. 5. Compromised mobility and viability of aging *dhtt-ko* mutants. (A) Spontaneous locomotion assay. *dhtt-ko* mutants show normal mobility at day 15 but older animals show significantly reduced mobility. (B) Age-dependent survival rate of adult animals. *dhtt-ko* mutants have a reduced life span. Both the mobility and viability defects in *dhtt-ko* mutants were rescued by the presence of a *dhtt* genomic minigene construct ('*dhtt-ko* Rescue'). Flies were collected from at least three different batches. The total number of flies counted for viability quantification were: wild type, *n*=659; *dhtt-ko*, *n*=1573; *dhtt-ko* Rescue, *n*=804; *elav-Gal4/+*; *dhtt-ko*, *n*=550. The difference between wild-type and *dhtt-ko* flies is statistically significant, *P*=0.0001, Student's *t*-test. The difference between wild-type and *dhtt-ko* Rescue flies is not statistically significant, *P*=0.36. The difference between wild-type and *elav-Gal4/+*; *dhtt-ko* flies is statistically significant, *P*<0.00001. The data in (A,B) are presented as the means±s.e.m. (C) RT-PCR analysis confirmed that expression of endogenous *dhtt* was lost in *dhtt-ko* mutants (lane 3) but was restored by the presence of the *dhtt* genomic minigene rescue construct (lane 4), similar to that in wild-type controls (lane 2). RT-PCR was performed on total RNA samples extracted from adult animals of each of the indicated genotypes. Primers for RT-PCR were located in adjacent exons in the control *rp49* gene (the group of four wells on the left) or in neighboring exons at the N-terminal (targeting exons 5 and 6, *dhtt*-N), middle (targeting exons 13 and 15, *dhtt*-M) and C-terminal (targeting exons 23 and 24, *dhtt*-C) regions of the *dhtt* gene (see Methods). The lane 1s are controls of PCR products from a wild-type genomic DNA template using these primer pairs, which are longer than the RT-PCR products generated by the same pair of primers owing to the spliced-out introns, thus confirming that RT-PCR products were indeed amplified from transcribed RNA templates. w^{1118}: wild-type control.

7). Among the A307-Gal4 labeled neurons, one pair, located at the dorsal-lateral edge of the brain, projects a prominent axon tract along the dorsal-posterior surface to the dorsal-central region of the brain, forming extensive dendritic connections (Fig. 7B-D; supplementary material Fig. S4). These neurons further extend their projections anteriorly, establishing a complex axon terminal structure with extensive varicosities and fine branches above the antennal lobe region of the brain (Fig. 7E,F,K; supplementary material Fig. S4). In *dhtt-ko* mutants, the axonal projections of A307-positive neurons follow the same path and their axons terminate at similar locations to those in wild-type flies; this is consistent with the observation that *dhtt* does not affect axonal integrity or pathfinding (Fig. 7G,H). Interestingly, axonal termini from both wild-type and *dhtt-ko* flies show a similar age-dependent maturation process, whereas axonal termini in young adult brains are mainly composed of a network of variable thin branches with no clearly recognizable synaptic boutons (supplementary material Fig. S4C,F) (3-day-old flies). Mature boutons develop as the animals age, with many prominent boutons being easily identifiable in the brains of 40-day-old flies (Fig. 7F,I; compare with supplementary material Fig. S4C,F). Owing to the significant variation in their structure and the lack of recognizable boutons, it is difficult to directly quantify and compare the size of these axonal termini in young adults. However, in aged *dhtt-ko* mutants, it is apparent that the axonal termini contain a significantly reduced number of varicosities and branches (Fig. 7H,I,N). Quantification of the total area covered by each axonal terminus revealed that the A307-positive axonal termini in 40-day-old *dhtt-ko* mutants cover about half of the area compared with controls (Fig. 7R) (average area covered by each axonal terminus: wild-type control=168.7±8.0 μm^2, *dhtt-ko* mutant=86.1±7.2 μm^2; *P*<0.0001; total number of A307-positive axonal termini quantified: wild-type control, *n*=18; *dhtt-ko* mutants, *n*=17). To rule out the possibility that this reduced complexity was because of the accelerated aging process or a secondary effect associated with the reduced mobility of *dhtt-ko* mutants, we examined the axonal termini of the A307-positive neurons in 83-day-old wild-type flies, as animals at this age are near the end of their life span and have severely reduced mobility. The structure of the axonal termini in these flies is similar to that of 40-day-old flies and shows no obvious reduction in terminal complexity (supplementary material Fig. S5).

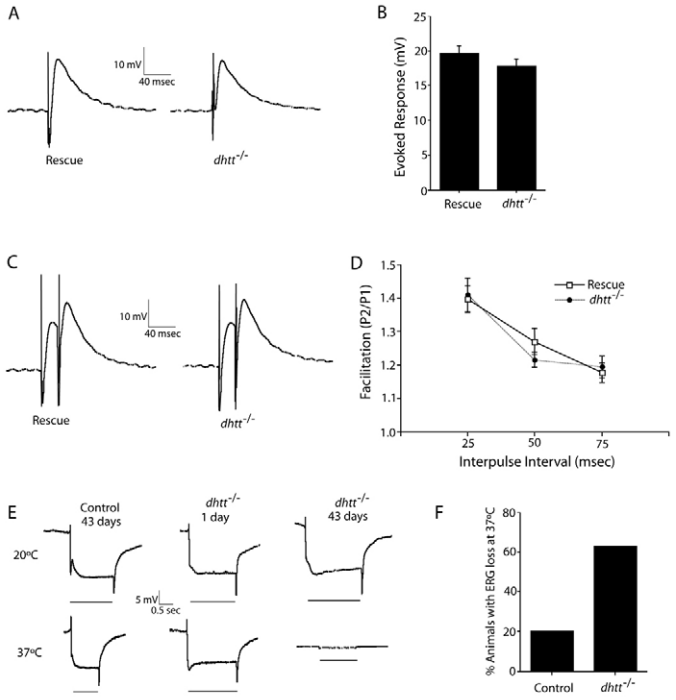

Fig. 6. Normal synaptic transmission in *dhtt-ko* mutants.
(A-F) Electrophysiological analyses of *dhtt* mutants (see Methods). (A) Voltage traces of evoked EJPs recorded from muscle fiber 6 in *dhtt* mutant or control third instar larvae. (B) Measurements of evoked EJP amplitude. The *dhtt-ko* mutants exhibited no significant difference in synaptic vesicle release following stimulation (P=0.18, Student's t-test). Resting membrane potential was unchanged in animals lacking *dhtt*. (C) Voltage traces and (D) quantification of PPF in control and *dhtt* mutant third instar larvae. No change in the amplitude of PPF was observed in *dhtt* mutants, indicating that short-term plasticity is intact. (E) ERGs recorded from controls and *dhtt-ko* mutants aged 40-45 days or from *dhtt-ko* mutants aged 1-3 days at 20°C (top graphs) or at 37°C (bottom graphs); heat pulses were given at regular intervals. The black bar below the trace indicates the test light pulses. (F) Percentage of adult animals aged 40-45 days with a loss of phototransduction at 37°C. *dhtt-ko* mutants showed a more severe temperature-induced loss of phototransduction than control flies, suggesting that photoreceptors in aged *dhtt-ko* mutants were stress-sensitive compared with the controls. The *dhtt-ko* Rescue animals were used as controls in the above electrophysiological analyses to ensure a consistent genetic background (A-F). The data in (B) and (D) are presented as the means±s.e.m.

Using the membrane-bound mCD8-eGFP reporter driven by the GF-specific A307-Gal4 line, we further analyzed the axonal projection and terminal morphology of the GF neurons in *dhtt-ko* mutants. The GF neurons are a pair of large interneurons located in the central brain and project their prominent axons, which are unbranched, to the mesothoracic neuromere (T2) in the ventral nerve cord, where they bend laterally and synapse with other interneurons and motor neurons (Phelan et al., 1996). In both young (3-day-old) and aged (40-day-old) *dhtt-ko* mutants, GF neurons project normally to the T2 neuromere and form the characteristic terminal bends, resembling those observed in wild-type controls (supplementary material Fig. S6). In 3-day-old animals, the signal intensity of the mCD8-eGFP reporter at the GF axonal termini was similar between *dhtt-ko* mutants and wild-type controls (supplementary material Fig. S6B,C) (total number of 3-day-old GF axonal termini examined: wild-type control, n=10; *dhtt-ko* mutants, n=12). However, in 40-day-old animals, the GF axonal termini in wild-type controls showed a much stronger enrichment for the mCD8-eGFP reporter than in *dhtt* mutants (supplementary material Fig. S6D-G) (total number of 40-day-old GF axonal termini examined: wild-type control, n=16; *dhtt-ko* mutants, n=20). The exact nature behind such a difference remains to be clarified, but might represent subtle alterations in axonal transport of membrane proteins in aged neurons. Nevertheless, these results suggest that *dhtt* does not affect axonal pathfinding and overall brain organization, but has a functional role in regulating the complexity of axonal termini in the adult brain.

Loss of *dhtt* enhances the pathogenesis of HD flies

Earlier studies in cell culture and *Htt* mutant mice have shown that wild-type Htt has a protective role for CNS neurons (Dragatsis et al., 2000; O'Kusky et al., 1999; Rigamonti et al., 2000; Van Raamsdonk et al., 2005). Further, existing evidence suggests that normal Htt activity can be inactivated by mechanisms such as abnormal sequestration into insoluble aggregates (Huang et al., 1998; Kazantsev et al., 1999; Narain et al., 1999; Preisinger et al., 1999; Wheeler et al., 2000). These and other observations have lead to the hypothesis that the perturbation of endogenous Htt function, such as by late-onset inactivation of endogenous Htt, contributes to HD pathogenesis (Cattaneo et al., 2001). Attempts to test this directly in mouse Hdh mutants have been complicated by the crucial role of Hdh in early mouse embryogenesis and in the later stages of brain development (Auerbach et al., 2001; Dragatsis et al., 2000; Duyao et al., 1995; Leavitt et al., 2001; Nasir et al., 1995; Van Raamsdonk et al., 2005; White et al., 1997; Zeitlin et al., 1995). However, we have a unique opportunity to examine this in Drosophila because *dhtt* is not essential for fly embryogenesis and *dhtt* mutants appear to behave normally at young ages, with only a mild axon terminal defect in the brain. We used a well-established fly HD model for polyQ toxicity (HD-Q93), in which the human *HTT* exon 1, with 93 glutamine repeats, is expressed in all neuronal tissues (genotype: *elav-Gal4/+*; *UAS-Httexon1-Q93/+*) (Steffan et al., 2001). The HD-Q93 flies develop age-dependent neurodegenerative phenotypes in adults, which manifest as initial hyperactivity followed by a gradual loss of coordination and a decline in locomotor ability, with eventual death at around 20 days of age (Fig. 8F-H). The HD-Q93 flies also develop a progressive degeneration of both the brain and other neuronal tissues, most prominently in the photoreceptor cells in the eye (Steffan et al., 2001).

After introducing HD-Q93 into the *dhtt* mutant background ('HD-Q93; *dhtt-ko*' flies; genotype: *elav-Gal4/+; UAS-Httexon1-Q93/+; dhtt-ko/dhtt-ko*), we examined the eye degeneration phenotype by quantifying the number of rhabdomeres in each ommatidia as the animals age. The loss of photoreceptor cells in HD-Q93 flies was not significantly enhanced in the absence of endogenous *dhtt* (Fig. 8A-E). For example, at 11 days of age, approximately 40% of ommatidia lost three photoreceptors in both HD-Q93 and HD-Q93; *dhtt-ko* flies (Fig. 8E) (number of ommatidia with four photoreceptors: HD-Q93=42.6±2.9%, n=562, eight adult eyes analyzed; HD-Q93; *dhtt-ko*=37.6±4.1%, n=266, seven adult eyes analyzed; the difference was statistically insignificant, P>0.5).

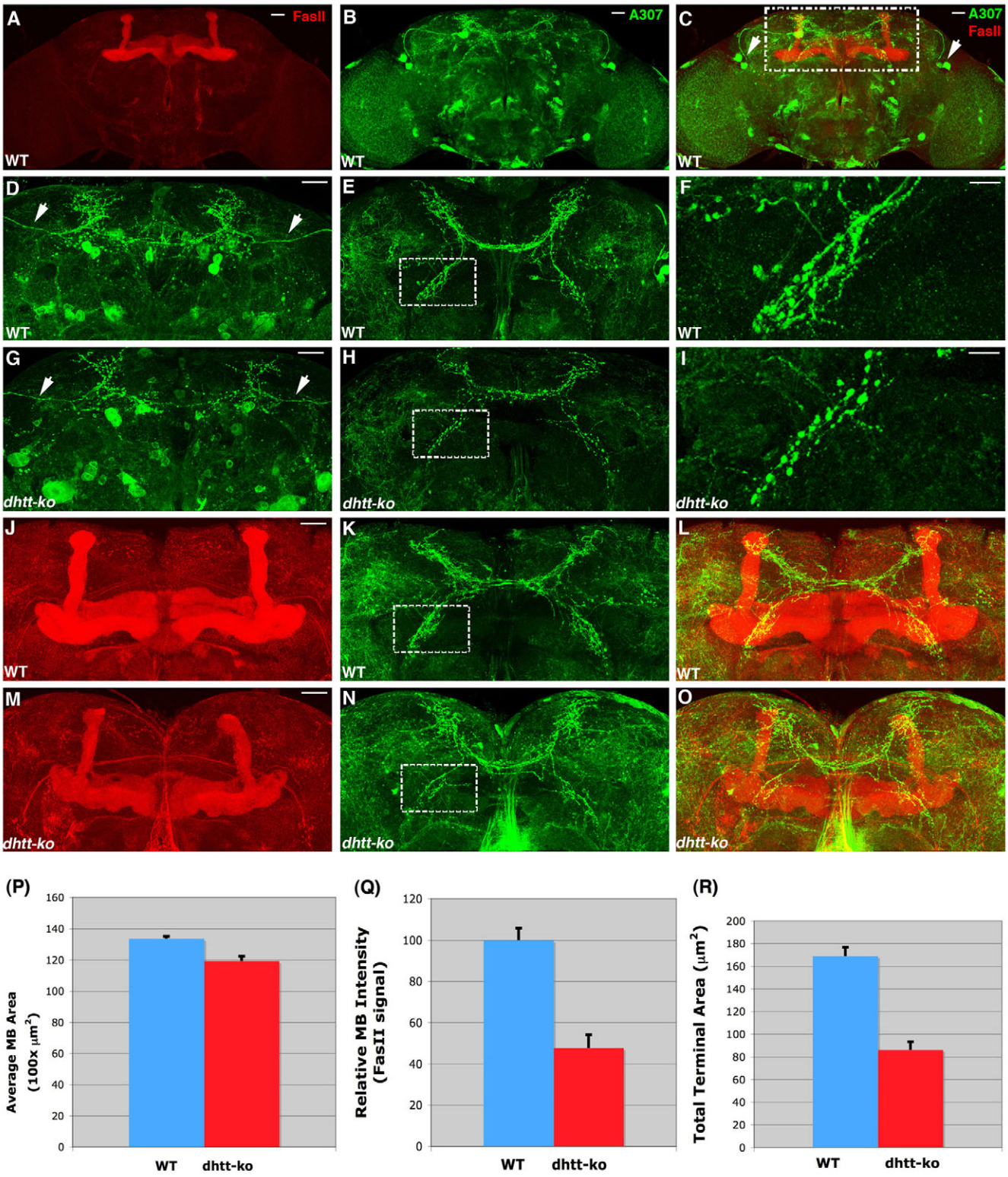

Fig. 7. See next page for legend.

Further, the overall profile of the remaining photoreceptors per ommatidia was also similar between these flies (Fig. 8E).

Interestingly, although these HD-Q93; *dhtt-ko* flies showed normal mobility at the beginning of their adult life, they displayed a declining mobility that could be detected as early as 5 days of age and that rapidly deteriorated over the next few days (supplementary material Movies 4-8). During this time, the flies become progressively uncoordinated, showing an increasing frequency of

Fig. 7. Reduced complexity of axonal termini in *dhtt-ko* brains. (A-C) Brain morphology of a 40-day-old wild-type adult fly as revealed by anti-FasII staining (red) (A), which strongly labels the MBs. In the same brain, A307-positive neurons and their axonal projections are revealed by using a membrane-bound mCD8-eGFP reporter (green) (B). (C) An overlay of images (A) and (B) showing the relative positions of MBs and A307-positive neurons in the brain. A307-positive neurons with prominent axonal projections are highlighted [white arrows in (C)]. The white dashed lines delineate the region magnified in the following pictures (D-O). (D-I) Axonal projection patterns and axon terminal structures of A307-positive neurons in 40-day-old wild-type (D-F) and *dhtt-ko* mutant (G-I) brains. For clear visualization, the posterior (D,G) and anterior (E,H) of the brains are projected separately. (D,G) A307-positive neurons have a similar axonal projection pattern (white arrows) in *dhtt-ko* mutant (G) and control brains (D). (E,H) Anterior views of the same brain regions showing the axon terminal structure. The white dashed lines border one axon terminus in each brain, which are further magnified in (F) and (I), respectively. Notice the significant reduction in branching and varicosities at the axonal termini of the *dhtt-ko* mutant (H,I). (J-O) The MBs (J,M) and axonal termini of A307-labeled neurons (K,N) in another pair of 40-day-old wild-type (J-L) and *dhtt-ko* mutant (M-O) brains. (M) The overall morphology of the MBs is normal but the signal intensity is weaker in the *dhtt-ko* mutant. The white dashed lines border one axon terminus in each brain. Note the reduced complexity of axonal termini in the *dhtt-ko* mutant. The top of each image is the dorsal end of the brain. WT=w^{1118} wild-type control. Bars, 10 μm (F,I) and 30 μm (all other panels). (P,Q) Quantification of the average area covered by each MB (P) and the relative signal intensity of MBs (Q) between wild-type controls (WT, blue) and *dhtt-ko* mutants (red), as revealed by anti-FasII staining. When calculating the relative signal intensity of MBs, the value for the average signal intensity from the wild-type controls was set as 100, (s.e.m.=5.8); the relative signal intensity of the *dhtt-ko* mutants=47.7±6.1; $P<0.0001$. (R) Quantification of the average total area covered by each A307-positive axonal terminus. The genotypes of each fly line tested are indicated under each chart. WT=w^{1118} wild-type control. The data in (P-R) are presented as the means±s.e.m.

both faltering while walking and falling during climbing (Fig. 8G; supplementary material Movies 4-8). In a standard climbing assay, almost all 3-day-old HD-Q93; *dhtt-ko* flies could successfully climb to the top of a vial, which is similar to that observed for wild-type controls. However, by day 11, only around 10% of viable HD-Q93; *dhtt-ko* flies could make it to the top, whereas the success rate was 61% for HD-Q93 flies, and more than 94% for wild-type and dhtt-ko flies (Fig. 8F) [based on an average of at least five independent assays of 20 flies for each genotype at the given age; compared with wild-type controls on day 11, the results from *dhtt-ko* flies were not significant ($P=0.30$), whereas the results from HD-Q93 and HD-Q93; *dhtt-ko* flies were significant ($P<0.0001$)]. Similarly, when spontaneous locomotion was tested, the HD-Q93; *dhtt-ko* flies showed a more rapid decline in motility over time, and by day 9, these flies were less than half as active as those in the other groups (Fig. 8G) (activity was measured by the number of spontaneous turns performed every 4 minutes; on day 9, HD-Q93; *dhtt-ko*=26.4±5.9, $n=9$; HD-Q93=66.5±5.0, $n=8$; elav-Gal4; *dhtt-ko* control=60.6±4.3, $n=9$; UAS-Httex1Q93; *dhtt-ko* control=66.2±3.0, $n=9$; the HD-Q93; *dhtt-ko* results were statistically significant when compared with UAS-Httex1Q93; *dhtt-ko* control flies, $P=0.00002$). Furthermore, the life span of *HD-Q93; dhtt-ko* flies was shortened significantly, with half of them dying by day 8 and almost all of them by day 14. In contrast, only about 7% of the HD-Q93 flies died at day 8 and half of them by day 14 (Fig. 8H) [viability at day 8: HD-Q93; *dhtt-ko*=45.0±3.2%, $n=409$ (from four different crosses); HD-Q93=93.1±1.7%, $n=1082$ (from eight different crosses); the difference between HD-Q93 and HD-Q93; *dhtt-ko* flies was statistically significant, $P=0.0003$]. Notably, at day 15, *dhtt-ko* mutants were healthy and displayed similar mobility to wild-type controls (Fig. 5A,B).

To understand the underlying pathology of these phenotypes, we further examined the brain structure of these flies. Compared with HD-Q93 flies of the same age, the brains of HD-Q93; *dhtt-ko* flies had already developed a more severe pathology at 5 days. Notably, the MBs appeared less organized – the characteristic bulged tip of the vertical α-axonal lobes, which were prominent in HD-Q93 flies (Fig. 9C, white arrows) ($n=14$) and other controls, was largely unrecognizable in 95% of HD-Q93; *dhtt-ko* flies ($n=17/18$) (Fig. 9H, white arrows) (supplementary material Figs S7 and S8). The clear separation, along the midline, between the pair of medially projected β-lobes, which was obvious in HD-Q93 flies (Fig. 9C, white arrow) (supplementary material Figs S7 and S8) ($n=14$) and wild-type flies (Fig. 7J), also became less distinct and often appeared to be merged in HD-Q93; *dhtt-ko* flies ($n=13/18$) (Fig. 9H, white arrow) (supplementary material Figs S7 and S8). In addition, the anti-FasII staining of the MBs was not as strong in HD-Q93; *dhtt-ko* flies as in HD-Q93 flies (Fig. 9C,H; supplementary material Figs S7 and S8). Quantification of MB size and FasII staining signals revealed that there was approximately a 7% reduction in the average size of MBs in HD-Q93; *dhtt-ko* mutants compared with HD-Q93 controls (Fig. 9K). The γ-lobe signals were too weak to be reliably tracked in both HD-Q93 and HD-Q93; *dhtt-ko* flies, so only the α- and β-lobes in each MB were measured (average MB size: HD-Q93=11,137±314 μm^2, $n=6$; HD-Q93; *dhtt-ko*=10,412±212 μm^2, $n=7$; $P=0.04$). The average signal intensity of FasII signals in the MBs of *dhtt-ko* mutants was also decreased, by around 31% (Fig. 9L) (relative signal intensity of α- and β-lobes in the MBs: HD-Q93=100±6.7 μm^2; *dhtt-ko* mutant=69.3±4.0 μm^2; $P=0.0004$). Furthermore, the HD-Q93; *dhtt-ko* brains showed larger areas that were devoid of neuronal cells (compare Fig. 9A and 9D with Fig. 9F and 9I, respectively; also see supplementary material Figs S7 and S8). The results obtained from quantifying the brain size of these flies suggested that, although the overall size of the brains was similar between HD-Q93 and HD-Q93; *dhtt-ko* flies (Fig. 9M) (average brain size: HD-Q93=119,279±2015 μm^2, $n=7$; HD-Q93; *dhtt-ko*=115,389±2412 μm^2, $n=7$; $P=0.003$), the total area that was devoid of neuronal cells was increased by about 25% (Fig. 9N) (total area devoid of neurons cells: HD-Q93=26,324±1869 μm^2, $n=7$; HD-Q93; *dhtt-ko*=32,945±2494 μm^2, $n=7$; $P=0.03$). Together, these results suggest that there is increased disorganization and an increase in neuronal loss in the brains of HD-Q93; *dhtt-ko* flies. Thus, loss of endogenous *dhtt* renders animals more vulnerable to the toxicity associated with polyQ-expanded Htt.

DISCUSSION

Htt has been characterized extensively in mammalian cell culture and in mouse systems (Cattaneo et al., 2001; Harjes and Wanker, 2003). However, only a few functional studies have been performed on its homologs in other model organisms. By deleting the *dhtt* gene, we demonstrate that Htt is not required for normal development of Drosophila, but instead has an essential role for the long-term mobility and survival of adult animals. Subsequent

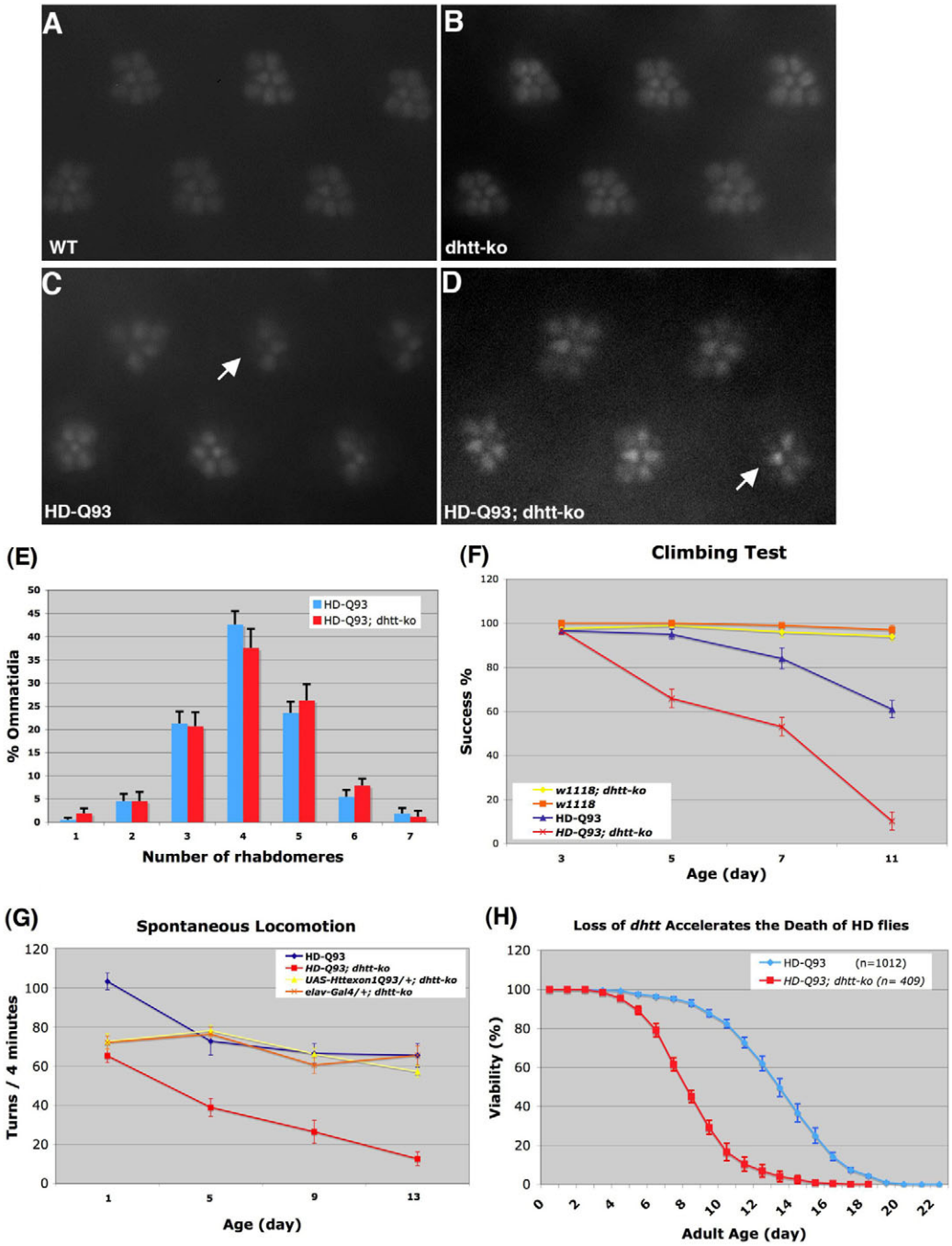

Fig. 8. Loss of endogenous *dhtt* enhances the mobility and viability phenotypes of HD flies. (A-D) Retinal organization, as revealed by pseudopupil imaging of 7-day-old adult eyes. Both wild-type (A) and *dhtt-ko* flies (B) had well-patterned ommatidium with seven rhabdomeres in each. Adult eyes from HD-Q93 (C) and HD-Q93; *dhtt-ko* (D) flies both showed an extensive loss of photoreceptors (arrows highlight ommatidia with only three or four rhabdomeres). (E) Histogram showing the number of remaining photoreceptors per ommatidium in 11-day-old adults. A similar profile of degeneration was observed for HD-Q93 flies (red) and HD-Q93; *dhtt-ko* flies (blue). (F-H) Quantification of climbing ability (F), spontaneous locomotion (G) and age-dependent survival rate (H). The genotypes for each of the fly lines tested are provided within each chart. HD flies with a background *dhtt-ko* mutation show an accelerated loss of mobility (F,G) and earlier lethality (H). The data in (E-H) are presented as the means±s.e.m.

analyses revealed that loss of *dhtt* mildly affects the integrity of adult brains. Further, in the absence of endogenous *dhtt*, the neurodegenerative phenotypes associated with a Drosophila model of polyQ toxicity were enhanced significantly.

The role of *Htt* homologs in animal development

Earlier studies showed that mice lacking *Htt* die during early embryogenesis (Duyao et al., 1995; Nasir et al., 1995; Zeitlin et al., 1995). It is surprising to find that *dhtt* is dispensable during Drosophila development. As no other Htt homolog exists in the fly genome (Li et al., 1999), such a mild phenotype is unlikely to be caused by a functional redundancy resulting from another *Htt*-like gene in Drosophila. Considering the evolutionary distance between Drosophila and mammals, such an observation might indicate that the Drosophila and mammalian Htt proteins, with their relatively restricted sequence homology, are not functionally conserved. However, this phenotypic discrepancy might also reflect intrinsic differences during mouse and fly embryogenesis. In a chimeric analysis of *Htt* mutant mice, Dragatsis et al. showed that the early embryonic lethality of *Htt*-null mice was primarily the result of a crucial role of Hdh in extraembryonic membranes (Dragatsis et al., 1998). It is probable that Drosophila does not

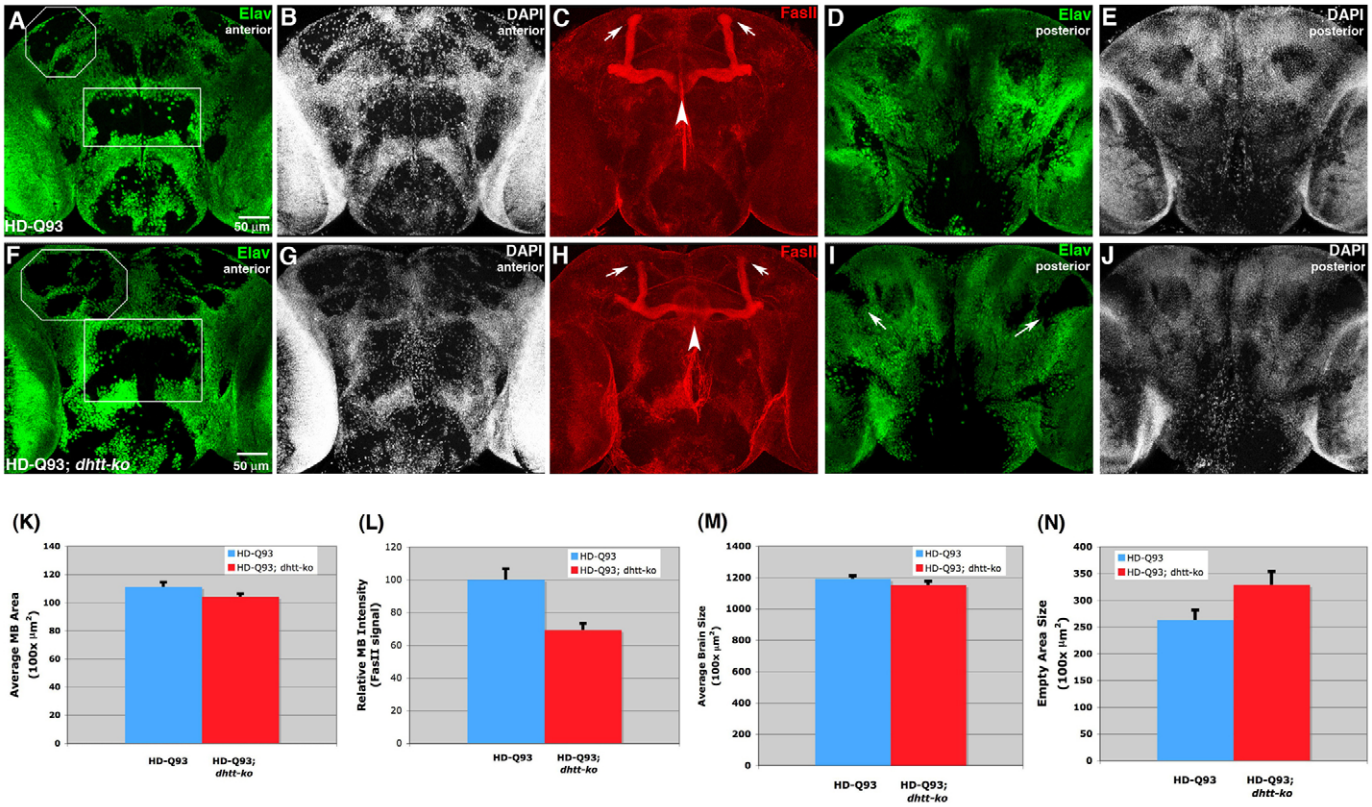

Fig. 9. Loss of endogenous *dhtt* affects the pathogenesis of HD flies. (A-J) Loss of endogenous *dhtt* causes enhanced brain pathology in HD flies. Confocal images of adult brains showing the distribution of neuronal cells (anti-Elav, green), cell nuclei (DAPI, white) and MBs (anti-FasII, red) in 5-day-old HD-Q93 (D-H) and HD-Q93; *dhtt-ko* (I-M) brains. As cells in the fly brain are mainly localized at its surface, the anterior (A,B,F,G) and posterior (D,E,I,J) halves of the brains are projected separately for better visualization of the distribution pattern. Note the enlarged regions devoid of neuronal cells in the HD-Q93; *dhtt-ko* brain (F) (the areas within the white lines) compared with the corresponding regions in the HD-Q93 brain (A). The arrows in (I) indicate the areas lacking neuronal cells at the posterior of the brain. (C,H) The MB in the HD-Q93*; dhtt-ko* brain (H) is also less well organized and shows weaker signal intensity than in the HD-Q93 brain (C). The white arrowheads highlight the clear separation, along the midline, between the two medial β-lobes in the HD-Q93*; dhtt-ko* brain (C), this is less distinct and appears merged in the HD-Q93 brain (H). White arrows indicate the bulged tip of the vertical α-lobes, which become less distinct in HD-Q93; *dhtt-ko* brains (H). WT=w^{1118} wild-type control. Bars, 50 µm (all panels). (K,L) Quantification of the average MB size (K) and relative signal intensity (L) of MBs in HD-Q93 (blue) and HD-Q93; *dhtt-ko* mutants (red), as revealed by anti-FasII staining. In both HD-Q93 and HD-Q93; *dhtt-ko* flies, the FasII signals for the γ-lobe in MBs were too weak to be tracked reliably (see supplementary material Figs S7 and S8); therefore, only the α- and β-lobes in each MB were measured. (M,N) Quantification of the average brain size (M) and the total size of the regions devoid of neuronal cells in the anterior brain (N), as revealed by using neuronal-specific staining with an antibody against Elav. The data in (K-N) are presented as the means±s.e.m.

require equivalent tissues, such as extraembryonic membranes, to support its early development and that its embryogenesis can proceed normally in the absence of *dhtt*. Although an Htt homolog is found in Drosophila and vertebrates, no Htt homolog has been found in yeast or *C. elegans* (Li et al., 1999). The absence of an Htt homolog in *C. elegans* suggests that Htt does not have a function that is essential for the development of invertebrates in general, which is in agreement with our observation that *dhtt* is dispensable for normal development of Drosophila. Interestingly, a phylogenetic comparison of Htt proteins from different species postulates that Htt in the protostome (which includes Drosophilids) might be dispensable because, when compared with the deuterostome branch, evolution of the *Htt* genes along the protostome branch is more heterogeneous (Tartari et al., 2008). Further studies will be required to determine whether the mammalian *Htt* gene can rescue Drosophila *dhtt*-null phenotypes.

Analyses of *dhtt-ko* mutants suggest that loss of *dhtt* does not affect synapse formation, neurotransmission or axonal transport (Figs 3-6), which is in agreement with the absence of an Htt homolog in the worm, in which the essential components of these cellular processes are conserved. It is possible that Htt still regulates these cellular processes, but with a minor role. Extrapolating, there is a possibility that the function of Htt is associated with a novel cellular process and/or animal function that has been acquired during evolution. For example, although *dhtt* is dispensable for Drosophila development, it is important for maintaining the long-term mobility and viability of adult animals (Figs 5 and 6). Compared to the worm, Drosophila has a relatively long life span, a more complex nervous system and a more active life cycle, raising an intriguing possibility that the function of Htt might be directly related to these higher functions in adult animals.

The role of Htt in adult brain

Although *dhtt* is dispensable for normal Drosophila development, *dhtt* mutants show significantly reduced mobility and viability as they age, indicating an important role of *dhtt* in maintaining the long-term functioning and survival of adult animals (Fig. 5). Analysis of *dhtt* mutants revealed a mild abnormality in MB structure and a reduction in the complexity of axonal termini in the brain (Fig. 7). Similarly, *Htt* mutant mice with a reduced level of Htt expression display severe brain abnormalities, even though non-neuronal tissue forms normally (White et al., 1997). Targeted inactivation of Hdh in the mouse forebrain also causes a progressive neurodegeneration phenotype, suggesting that Hdh is required in the development and survival of neuronal cells (Dragatsis et al., 2000). It remains to be determined whether common underlying molecular mechanisms are responsible for the observed brain phenotypes in the fly and mouse. Nonetheless, considering the evolutionary distance between Drosophila and the mouse, the existence of structural defects in the adult brain in both species could indicate a conserved role of Htt in maintaining neuronal integrity.

The axonal terminal phenotype in *dhtt* mutants is also reminiscent of that observed in a mouse knockout model for Htt (Hdh^{ex5}), in which exon 5 has been deleted (Nasir et al., 1995). Although mice homozygous for this Hdh deletion are early embryonic lethal, Hdh^{ex5} heterozygotes survive to adulthood and display increased neuronal loss, motor and cognitive deficits, and a significant loss of synapses in specific regions of the brain (Nasir et al., 1995; O'Kusky et al., 1999). Synapse complexity can be modulated by many factors, including neuronal activity and membrane and cytoskeleton dynamics. In the future, many questions remain to be answered, such as the significance of this axonal terminal phenotype, the exact function of Htt in axonal termini complexity and the possibility of a causal link between this brain defect and the observed adult mobility and viability phenotypes.

The role of endogenous *dhtt* in HD pathogenesis

Extensive studies on HD and other polyQ diseases have demonstrated that an expanded polyQ tract can itself be neurotoxic (Zoghbi and Orr, 2000). Given that the distinctive neuronal loss observed in each polyQ disease is caused by otherwise unrelated disease genes that are widely expressed, it has been hypothesized that other cellular factors affect disease pathogenesis (Cattaneo et al., 2001; Zoghbi and Orr, 2000). In HD, accumulating evidence from cell culture and mutant mouse studies suggest that wild-type Htt has a neuroprotective function (Cattaneo et al., 2001). When endogenous wild-type Hdh is replaced by yeast artificial chromosomes (YACs) containing full-length human Htt with an expanded polyQ tract (YAC46, YAC72 and YAC128) (Leavitt et al., 2001; Van Raamsdonk et al., 2005), the mice develop massive cell death in the testes that can be suppressed by the wild-type *Hdh* gene, suggesting that the normal function of Htt might mitigate the cellular toxicity associated with the polyQ-expanded mutant Htt protein (Leavitt et al., 2001; Van Raamsdonk et al., 2005). In addition, a genome-wide study of HD animal models and postmortem tissues has shown that neuronal genes regulated by the transcriptional repressor REST/NRSF, including the gene encoding BDNF, could be similarly repressed by either the presence of the polyQ-expanded Htt protein or by depleting endogenous wild-type Htt (Zuccato et al., 2007). Together, these and other studies support the hypothesis that loss of normal Htt function affects HD pathogenesis.

We were able to examine the effect of removing endogenous *dhtt* on the pathogenesis of an established Drosophila HD model for polyQ toxicity (HD-Q93). Our results show that the phenotypes of HD-Q93 flies, including mobility, viability and brain pathology, are significantly exacerbated in the absence of endogenous *dhtt,* providing in vivo evidence that loss of normal Htt function can accelerate HD pathogenesis. It should be noted that our results do not directly demonstrate that loss of the endogenous Htt protein specifically affects HD pathogenesis, because the enhanced pathology might be the result of an additive effect of two detrimental factors in the animals, namely the presence of a toxic polyQ tract and the disturbance of the normal function of Htt. Although *dhtt-ko* mutants exhibit only a mild age-dependent adult phenotype, it is possible that, in the absence of endogenous *dhtt*, some undetected cellular defects might develop that render the animals more susceptible to other cellular attacks. In the presence of a toxic polyQ tract, this vulnerability might be exposed further, leading to additive phenotypes. Our result is in agreement with the early hypothesis that HD might be caused by the combination of an acquired toxicity, conferred by the expanded polyQ tract in the mutated Htt, and an incurred neuronal vulnerability, arising from the loss of endogenous Htt function (Cattaneo et al., 2001). It is important to note that previous studies have demonstrated that expansion of polyQ tracts within the Htt protein does not abolish its endogenous function, as full-length Htt with an expanded polyQ tract can fully support the development of *Htt*-null mice (Leavitt et al., 2001; Van Raamsdonk et al., 2005; White et al., 1997).

Recently, RNAi-mediated depletion of the polyQ-expanded Htt protein has been proposed as a therapeutic approach against HD (Farah, 2007). Our data, together with previous mammalian studies, suggest that the normal function of Htt has a conserved neuroprotective role in the brain and that its depletion could render neuronal cells more vulnerable to the toxicity associated with the polyQ tract (Auerbach et al., 2001; Cattaneo et al., 2001; Dragatsis et al., 2000; Leavitt et al., 2001). Application of such an RNAi-based strategy requires a consideration that the normal Htt function be preserved. Given the devastating consequence of fully progressed HD, together with the observations that *Htt*-null neurons can develop and survive in the adult mouse brain and that *dhtt-ko* animals are largely normal with only mild adult brain defects, our data indicate that the benefit gained from balanced administration of RNAi knockdown therapy in the adult brain might justify the relatively mild loss caused by depletion of the Htt-associated neuroprotective function.

METHODS

Drosophila stocks and genetics

Flies were maintained at 25°C and raised on standard Drosophila medium unless specified otherwise. To establish transgenic animals, DNA constructs were injected into w^{1118} embryos together with the pπ25.7wc helper plasmid to generate germ line transformation; transformants were then selected in the next generation, according to standard procedures. Unless specified otherwise, flies of the genotype w^{1118}/w^{1118} were used as controls in all assays because

the *dhtt-ko* mutant allele was generated from this w^{1118} genetic background during the genetic crosses.

The p-element line d08071, piggyBac insertional line f05417 and the FLP recombinase transgene line [genotype: *y, w, pCaspeR-(hs-flipase)*] were from Exelixis (Parks et al., 2004).

To analyze the A307-Gal4 labeled neurons in adult brains, flies with genotypes of *A307-Gal4/+; dhtt-ko/TM6C, Tb* and *UAS-mCD8-eGFP/+; dhtt-ko/TM6C, Tb* were generated and crossed together; their adult progenies carrying *A307-Gal4/UAS-mCD8-eGFP; dhtt-ko/dhtt-ko* were selected and analyzed. The controls were the progenies from crossing the A307-Gal4 line with the UAS-mCD8-eGFP line.

HD-Q93 flies were obtained by crossing the pan-neuronal line *elav*-Gal4 (C155) with the UAS-Httexon1-Q93 line (P468) provided generously by L. Thompson and J. L. Marsh, respectively (Steffan et al., 2001). To generate 'HD-Q93; *dhtt-ko*' flies, flies with genotypes of *elav-Gal4(c155)/+; dhtt-ko/TM6C, Tb* and *UAS-Httexon1-Q93/Cyo; dhtt-ko/TM6C, Tb* were established and then crossed together; adult progenies with the genotype of *elav-Gal4/+; UAS-Httexon1-Q93/+; dhtt-ko/dhtt-ko* were then selected and analyzed. Controls flies had the following genotypes: *elav*-Gal4 (C155)/+; *UAS-Httexon1-Q93/+*; *elav-Gal4 (C155)/+; dhtt-ko/dhtt-ko*; and *UAS-Httexon1-Q93/+; dhtt-ko/dhtt-ko*.

Genetics and molecular clonings to generate the *dhtt-ko* mutant allele

Generation of the *Df(98E2)* deletion

The *Df(98E2)* deficiency, in which both *CG9990* and *dhtt* are deleted, was generated by following the Flp-FRT-based procedure, as described previously (Parks et al., 2004). Briefly, the p-element line d08071 (inserted at the 5′ end of the neighboring *CG9990* gene) was crossed to virgin flies carrying an FLP recombinase transgene [genotype: *y, w, pCaspeR-(hs-flipase)*]. For the next generation (F1), the male progenies carrying both the d08071 and the hs-flipase lines were selected and mated with virgins carrying the f05417 line, inserted near the 3′ end of the *dhtt* gene. The progenies (i.e. the F1 flies) from the above crosses were heat-shocked at 37°C for 1 hour, 48 hours after egg-laying, and were then heat-shocked for a further 1 hour during each of the following 4 days. In the third generation (F2), the virgin females were collected and crossed to males carrying balancer chromosomes (*w; TM3, Sb/TM6B, Tb, Hu*). In the fourth generation (F3), progeny flies carrying the *Df(98E2)* deletion from the above crosses (between F2 flies) were selected based on their darker eye color, and crossed with flies carrying balancer chromosomes to establish individual fly lines. The presence of the deletion in these lines was confirmed by PCR analysis of extracted genomic DNA and by DNA sequencing.

Genomic rescue construct for *CG9990* gene

To generate the genomic rescue construct for the *CG9990* gene, a 24.7 kb genomic DNA fragment, covering the *CG9990* genomic region, was isolated from the bacterial artificial chromosome (BAC) clone BACR10P23 (CHORI) following double digestion with the restriction enzymes *Xba*I and *Xma*I. This 24.7 kb genomic DNA fragment starts at an *Xba*I site near the end of the neighboring *CG9989* gene, 2.66 kb from the inserted site of the p-element line d08071, and ends at the *Xma*I site within the second exon of the *dhtt* gene, thus covering the whole genomic region of the *CG9990* gene (Fig. 1B). To generate the *CG9990* rescue transgene, this 24.7 kb genomic DNA fragment was cloned into the *Not*I and *Sma*I sites in the pCaspeR-4 transgenic vector. The DNA for the pCaspeR-4–*CG9990* genomic rescue construct was injected into w^{1118} embryos and transformants were then selected following standard procedures. Three independent *CG9990* transgenic lines were established and then tested by crossing them into the *Df(98E2)* deletion.

Generating the *dhtt-ko* mutant allele

Flies with the *Df(98E2)* deletion, which removes both *CG9990* and *dhtt*, are homozygous lethal at the embryonic stage. Through genetic crossings, we reintroduced the *CG9990* genomic rescue transgene back into the *Df(98E2)* deletion background, generating fly lines that are defective at the molecular level for only the *dhtt* gene (referred to as *dhtt-ko* flies). Three independent genomic *CG9990* transgenic lines were tested by crossing them into the *Df(98E2)* deletion; all of them rescued the embryonic lethality of the *Df(98E2)* deletion, producing viable adults. Thus, *dhtt-ko* flies, which carry both the *Df(98E2)* and the *CG9990* transgene, are homozygous viable and can fully develop into adulthood, demonstrating that the lethality observed with the *Df(98E2)* deletion is caused by the loss of *CG9990*. To verify further that the *dhtt* gene is indeed deleted, as expected, in this *dhtt-ko* allele, we extracted genomic DNA from the homozygous *dhtt-ko* and wild-type control adults and performed Southern blots.

Southern analysis

Genomic DNA was extracted from the *dhtt-ko* adults or from control w^{1118} adults and digested with the restriction enzyme *Bam*HI. DNA fragments were separated on a 1% agarose gel and transferred onto a nitrocellular membrane, according to the standard protocol for Southern blotting. DNA fragments specifically targeting all exons of the *dhtt* gene were labeled with ^{32}P-dCTP using the Klenow polymerase and random-hexamer primer method (Amersham) and used as probe. Hybridization was performed overnight at 65°C and the fragments were subsequently washed with SDS/SSC buffers, following standard procedures for Southern blotting.

dhtt minigene rescue construct

The size of the genomic region covering *dhtt* is about 43 kb (Li et al., 1999), which is too large to be cloned into a transgenic vector by conventional approaches. Therefore, we engineered a *dhtt* minigene rescue construct that expresses full-length *dhtt* under the control of its own endogenous regulatory region. In Drosophila, the regulatory elements controlling the endogenous expression pattern of a gene are normally located at the 5′ region of the gene, within the upstream 5′ untranscribed region and in the first few introns. In addition, the expression level of a gene is also affected by its 3′ untranslated region. As a result, we isolated a 14.9 kb genomic DNA fragment from the BAC clone BACR10P23 (CHORI) following double digestion with the restriction enzymes *Xba*I and *Asc*I. The *Xba*I site was located at the end of the *CG9990* gene and the *Asc*I site was within the tenth exon of the *dhtt*-coding region, thus the DNA fragment covered all of the 5′ untranscribed region of the *dhtt* gene together with the first ten introns and exons of the gene. We also isolated a 1.2 kb genomic DNA fragment, by

double digestion with *Stu*I-*Eco*RI, that covers the 3′ end of the *dhtt* gene, including the last exon of *dhtt* and the remaining polyA sites and untranscribed region at the 3′ end of the gene. Next, we assembled and isolated a 6.6 kb *dhtt* cDNA fragment, by digestion with *Asc*I and *Stu*I, that covered most of the 3′ cDNA region of *dhtt*, from the single *Asc*I site within the tenth exon to the *Stu*I site within the last exon. The *dhtt* minigene rescue construct was generated by ligating and fusing, in frame, the three fragments that cover all of the *dhtt* regulatory and coding regions: (1) the 5′ 14.9 kb genomic DNA fragment that covered all of the 5′ untranscribed region of the *dhtt* gene, as well as the first ten introns and exons of *dhtt*; (2) the middle 6.6 kb of the *dhtt* cDNA fragment that covered from exon 10 to exon 29; and (3) the 3′ 1.2 kb genomic DNA fragment that covered exon 29 and the polyA sites at the 3′ end of the gene, as well as the remaining 3′ untranscribed region. The 22.7 kb *dhtt* minigene was cloned into the *Not*I and *Xba*I sites in the pCaspeR-4 transgenic vector. After generating transgenic flies with this *dhtt* minigene rescue construct, we crossed these animals into the *dhtt-ko* mutant background to test whether the mobility and viability phenotypes of *dhtt-ko* mutants could be rescued.

UAS-*dhtt* construct and transgenic animals

Based on the published *dhtt* cDNA sequence (Li et al., 1999), we isolated overlapping fragments covering the full-length of the *dhtt* cDNA by PCR amplification using Pfu polymerase. We then assembled a full-length *dhtt* cDNA construct using these sequencing-verified *dhtt* fragments, cloned it into a pUASP vector, and generated transgenic fly lines by following standard protocols.

RT-PCR analysis

Total RNA samples were isolated, using Trizol reagent (Invitrogen), from adult animals of the following genotypes: w^{1118} wild-type control, homozygous *dhtt-ko* mutants and *dhtt-ko* Rescue. RT-PCR reactions were performed using Superscript one-step RT-PCR with Platinum Taq (Invitrogen) following the manufacturer's instructions. PCR primers were designed as follows: rp49 control: forward (in exon 1 of *rp49*) 5′-ACCATCCGCCCAGCATACAGG-3′, reverse (in exon 2 of *rp49*) 5′-TTGGCGCGCTCGACAATC-TCC-3′; dhtt-N: forward (in exon 5 of *dhtt*) 5′-GCCAATGTA-GCCAGAGTCTG-3′, reverse (in exon 6 of *dhtt*) 5′-CGCATTC-GCTGATGCTGCGTG-3′; dhtt-M: forward (in exon 13 of *dhtt*) 5′-AAGCTATTCGAGCCGATGGTC-3′, reverse (in exon 15 of *dhtt*) 5′-GCACCAGGAATCTCAGCATGG-3′; dhtt-C: forward (in exon 23 of *dhtt*) 5′-TCGGGAATTGACTTTCGCAGC-3′, reverse (in exon 24 of *dhtt*) 5′-TGCAGTTTGAGGCAGCGTTCC-3′.

Analysis of HEAT repeats in Htt proteins

Using the motif-predicting program developed by M. A. Andrade at the EMBL (http://www.embl-heidelberg.de/~andrade/papers/rep/search.html), both dHtt and human Htt were analyzed for the presence of HEAT repeats. Using the default parameters at the site and including the AAA, ADB and IMB groups of HEAT repeats (Andrade et al., 2001), a total of 40 and 38 HEAT repeats were identified for Htt and dHtt, respectively.

Immunohistochemistry and imaging analysis

Sample preparation and staining for embryos, larval tissues and adult fly eyes have been described previously (Sullivan et al., 2000). To analyze NMJs, wandering third instar larvae were dissected in Ca^{2+}-free saline (128 mM NaCl, 2 mM KCl, 0.1 mM $CaCl_2$, 4 mM $MgCl_2$, 35.5 mM sucrose, 5 mM Hepes at pH 7.2, 1 mM EGTA) and stained, as described (Sullivan et al., 2000). 1-2 μM thin sections of embedded adult eyes were cut using a microtome and imaged directly without further dye staining.

To stain and image the adult brains, flies were dissected in 1×PBS or in Drosophila M3 medium, to remove cuticles and external eye tissues, then fixed in 4% formaldehyde in 1×PBS for 1 hour at room temperature (RT), washed six times with 1×PBT for 1 hour, and stained with primary and secondary antibodies.

Whole-mount RNA in situ

Collection and fixation of Drosophila embryos, larvae tissue dissection and fixation, as well as RNA in situ hybridization were carried out according to standard procedures (Hauptmann and Gerster, 2000). The DIG-labeled RNA probes were generated according to the manufacturer's instructions (Roche, Indianapolis, IN). The *dhtt* exon 8 and exon 20 sequences were used to generate *dhtt*-specific in situ probes, which gave similar in situ results. The samples for in situ hybridization were analyzed with a Zeiss Axiophot 2 compound microscope.

Antibodies

To generate the antibody against dHtt, a cDNA fragment corresponding to the N-terminal 459 amino acids of dHtt was cloned into the pGEX-4T1 vector; the corresponding GST-fusion protein was purified according to manufacturer's instructions (Promega) and used to produce polyclonal antibody in a rabbit (Convance). The antiserum was affinity-purified and used at a final dilution of 1:200.

Primary antibodies were applied at 4°C overnight at the following dilutions: rabbit anti-GFP (1:1000, Molecular Probes); rabbit anti-fasciclin II (1:400) and anti-DIG (1:40,000), both generously provided by Mary Packard and Vivian Budnik (Budnik et al., 1996; Koh et al., 1999); rabbit anti-synaptotagmin (1:500) (Littleton et al., 1993); mouse anti-α-tubulin (1:10,000, Sigma); monoclonal mouse anti-fasciclin II (1D4, 1:20), anti-DIG (1:20), anti-CSP (1:20), anti-synapsin (1:50), anti-α-spectrin (1:20), anti-Armadillo (1:100), nc-82 (1:50) and anti-Futsch (22C10, 1:100) (all from Developmental Studies Hybridoma Bank) (Hummel et al., 2000; Roos et al., 2000); goat anti-HRP (1:500, Jackson Labs); Alexa488-, Alexa594- and Alexa647-conjugated secondary antibodies (all used at 1:500, Molecular Probes). Rhodamine Red X-conjugated goat anti-HRP and CY5-conjugated secondary antibodies were used at 1:200 (both from Jackson Labs). DAPI (0.2 μg/ml, Molecular Probes) and TRITC-conjugated phalloidin (10 ng/ml, Sigma) were applied in PBS-Tween (PBST) for 30 minutes to label nuclei and F-actin, respectively.

Image analysis

To quantify MBs, adult brains were prepared for imaging as described above. Dissected adult brains from both wild-type controls and *dhtt-ko* mutants were stained side by side in a 12-well plate with mouse anti-Fas II antibody (1D4, 1:20) overnight at 4°C. After washing six times with 1×PBT for 2 hours, samples were stained with Alexa-594-conjugated secondary antibodies (1:500) at RT for 2 hours, followed by extensive washing with 1×PBST for 2

hours at RT. To ensure that the stained samples had a similar background signal during imaging analysis, brains from both wild-type controls and *dhtt-ko* mutants were mounted onto opposite ends of the same slide. The samples were photographed at 20× magnification, under the same optical parameters, using a Zeiss fluorescent microscope (Axioskop 2 Mot Plus). The boundaries of MBs were traced manually using AxioVision Rel 4.5 software (Zeiss), and both the overall size of each MB and the total intensity of FasII staining signals within the MB boundary were computed using the same software. FasII staining signals from outside the MB boundary were also measured and used as a reference to subtract out the background signals. Since we could not confidently measure the thickness of the MBs in these samples, only the overall area covered by each MB was measured. The average FasII signal intensity in each MB was calculated by dividing the 'total intensity of FasII staining signals within the MB boundary' by 'the overall size of the MB'. To calculate the relative signal intensity, the average signal intensity of FasII signals from all wild-type brains was calculated and its mean was set as a reference point of 100.

To measure the overall brain size and the regions that were devoid of neurons in the brain, adult flies were dissected and stained with rat anti-Elav antibody (1:40), which labels all neuronal cells. The boundary of the whole protocerebrum in the brain and the regions devoid of neurons were tracked manually and quantified with AxioVision Rel 4.5 software, as described above.

To quantify the size of the A307-positive axonal terminals, adult brains from both wild-type controls and *dhtt-ko* mutants were dissected, fixed and stained side by side with an anti-GFP antibody, as described above, then mounted on the two sides of the same slide to ensure that they had a similar background for imaging analysis. Both the wild-type control and *dhtt-ko* mutant samples were imaged by confocal microscopy at 40× magnification under the same optical parameters. A Z-serial section of confocal images covering the entire depth of each axonal terminus was collected using a Leica TCS confocal microscope and then projected into one merged image (using the Leica software) to generate the whole picture of each axonal terminus. Since the branches and boutons in the brain were too small to distinguish clearly, only the overall area covered by each axonal terminus was measured.

Fluorescent images were analyzed and captured by fluorescent microscopy (Axioskop 2 Mot Plus, Zeiss) or by confocal microscopy (Leica TCS SP2 AOBS system). Confocal images were analyzed and projected using Leica confocal software (LCS).

Viability assay

Drosophila viability was measured by placing 30 newly hatched female flies of each genotype into individual vials, containing fly food, at 25°C. The number of dead flies was recorded daily. Flies were transferred into a new food vial every 3-4 days to prevent them from sticking to old food. For each genotype, at least two independent cohorts of flies, raised at different times from independent crosses, were tested and the results were averaged.

Mobility tests of adult flies and videos

Female flies were chosen in all the mobility tests. Fly videos were captured using a Sony digital camcorder (DCR-TRV140) and edited in Apple's iMovie program.

Climbing assay

Climbing assays were performed as described previously (Ganetzky and Flanagan, 1978; Le Bourg and Lints, 1992). Briefly, 20 flies of a specified age were knocked to the bottom of a plastic vial. The number of flies that could climb to the top of the vial after 18 seconds was counted. The test was repeated 6-7 times for each genotype at the specified age.

Spontaneous locomotion assay

The assay was performed as described previously (Feany and Bender, 2000; Joiner and Griffith, 1999; Wang et al., 2004). For each genotype, 6-14 flies of a specific age were tested.

Paraquat test

Flies were fed 30 mM of methyl viologen (Sigma) in instant Drosophila medium (Carolina), providing a dosage of paraquat that kills about 50% of wild-type flies after 48 hours of exposure. Control flies were fed instant medium only. Adult flies that had eclosed within the last 24 hours were kept in 30 mM paraquat or in drug-free medium for 48 hours after eclosion. The number of survivors was counted at 48 hours after the start of paraquat treatment.

Electrophysiology analysis

An electrophysiological analysis of wandering-stage third instar larvae was performed in Drosophila HL3.1 saline (NaCl, 70 mM; KCl, 5 mM; $MgCl_2$, 4 mM; $CaCl_2$, 0.2 mM; $NaHCO_3$, 10 mM; trehalose, 5 mM; sucrose, 115 mM; HEPES-NaOH, 5 mM; pH 7.2) using an Axoclamp 2B amplifer (Axon Instrument) at 22°C. Recordings were performed at muscle fiber 6/7 of segments A3 to A5 under current clamp. PPF was measured by determining the peak amplitude responses (P2/P1) of two stimuli separated by the indicated latency. All error bars are s.e.m. In adults, extracellular field potentials were recorded by placing a sharp glass electrode near the longitudinal flight muscles after piercing the cuticle, with a reference electrode placed in the fly head. ERGs were performed as described previously (Rieckhof et al., 2003). Temperature shifts were performed by heating mounting clay, which encompassed the fly, to the desired temperature with a peltier heating device.

For measurements of evoked EJP amplitude (Fig. 6A,B), the number of NMJs examined were: control, n=8; *dhtt-ko*, n=23. Voltage traces of evoked EJPs were recorded from muscle fiber 6 in third instar larvae in 0.2 mM extracellular calcium. Average resting potential: 60.2±1.2 mV in control animals and 62.4±0.8 mV in *dhtt* mutants. Average EJP amplitude: 19.5±1.2 mV in control animals and 17.8±1.0 mV in *dhtt* mutants.

Measurements of voltage traces of PPF (Fig. 6C) were performed at 25 millisecond intervals in control (rescued) and *dhtt* mutant third instar larvae in 0.2 mM extracellular calcium. Quantification of PPF (the amplitude of EJP 2 divided by the amplitude of EJP 1) was performed in control and *dhtt* mutants for 25-, 50- and 75-millisecond intervals (Fig. 6D). The number of preparations analyzed were: control, n=9; *dhtt-ko*, n=8.

The GF flight circuit can be activated by stimulation of the brain, and extracellular recordings can be made from the DLMs. Neither the control nor the *dhtt-ko* mutants displayed abnormal activity in the DLM flight muscles (data not shown).

TRANSLATIONAL IMPACT

Clinical issue

Huntington's disease (HD) is a degenerative brain disorder affecting approximately 30,000 people in the USA alone. It is characterized by involuntary movements (chorea), psychiatric symptoms such as irritability and delusions, and memory loss. These symptoms are progressive causing eventual incapacity and death.

HD is caused by an expansion of a CAG trinucleotide repeat in a single gene called huntingtin (*HTT*). Normal individuals have fewer than 34 CAG repeats, whereas HD patients have more than 35. The repeat length correlates inversely with the age of disease onset. Each CAG encodes a glutamine (Q) residue, so the protein product from *HTT* in HD has a longer glutamine tract, also known as a polyQ tract. Studies in different model systems, including yeast, fruit flies and mice, show that an expanded polyQ tract is toxic to cells. In addition to HD, a further eight neurodegenerative diseases are now known to be caused by the expansion of CAG repeats in eight other unrelated genes. Although Htt and other polyQ proteins are expressed widely, each polyQ disease selectively affects distinct, largely non-overlapping populations of neurons in the brain, suggesting that altering the normal function of the polyQ genes contributes to disease pathogenesis. However, the normal cellular function of Htt is largely unknown and the study of Htt is impeded by the absence of a tractable genetic model, since mice lacking *Htt* die during early embryogenesis.

Results

In this study, the Drosophila *HTT* homolog (*htt*, hereafter referred to as *dhtt*) was removed from the fly genome and its effect on development and neuronal function was characterized. Like vertebrates, *Drosophila melanogaster* (i.e. the fruit fly) has a single *Htt*-like gene (*dhtt*) but, unlike vertebrates, flies lacking *dhtt* develop normally. The authors find that several cellular processes that are suspected to require the wild-type Htt protein, such as neuronal development, axonal vesicle transport and neuronal transmission, are not significantly affected by the loss of *dhtt*. Instead, *dhtt*-deficient flies display mild adult phenotypes, including reduced complexity of axonal termini in the adult brain, declining mobility with age, and a shortened life span. Furthermore, when an established fly HD model (transgenic flies expressing a mutated human Htt fragment with an expanded polyQ tract in the nervous system) was analyzed in the absence of endogenous *dhtt*, animals developed neurological symptoms (e.g. incoordination and shaking, and reduced activity and viability) much more quickly, suggesting a protective function of the wild-type *dhtt* gene.

Implications and future directions

This study demonstrates that the fruit fly *Htt* ortholog is required for maintenance of mobility and long-term survival of adult animals, and its activity affects the fine structure of axonal termini in the brain. This work also provides in vivo evidence that disruption of the normal function of the *Htt* gene enhances HD disease progression. Together with previous mammalian studies, these results imply that both the presence of mutant protein and the depletion of the normal protein contribute to HD pathology. However, this study suggests a therapeutic potential for partial depletion of the endogenous Htt protein, using RNA interference for example, since removing the fly *dhtt* gene has only mild effects. This fly model should lend itself to future understanding of the molecular events contributing to HD, such as the role of the wild-type Htt protein, and identify good target areas for therapeutic intervention.

doi:10.1242/dmm.003046

To measure ERGs at the elevated temperature (37°C), flies were rapidly heated from 20°C to 37°C, with test light pulses (black bar below trace in Fig. 6E) given at regular intervals. A total of ten *dhtt-ko* mutants, aged 1-3 days, were tested and all showed normal ERGs at 20°C and 37°C (Fig. 6E). The number of preparations for the 40–45-day-old animals analyzed was: control, n=10; *dhtt-ko*, n=16.

ACKNOWLEDGEMENTS

We thank Leslie M. Thompson and J. Lawrence Marsh for providing advice and Drosophila stocks; Mary Packard for critical discussions and for generously providing experimental materials and technical help; Pengyu Hong for helping to quantify the size of the A307-positive axonal termini; Bun Chan for assistance in capturing and editing videos; Rodney Stewart, Richard Binari, Bernard Mathey-Prevot and Carl Johnson for advice and critical reading of the manuscript; and members of the Perrimon lab for their assistance, in particular Jianwu Bai for assistance in muscle analysis and Christian Villalta for fly injections. We thank the anonymous reviewers for their insightful comments. S.Z. gratefully acknowledges support in the form of a fellowship from the Harvard Center for Neurodegeneration and Repair (HCNR), as well as the Lieberman Award from the Hereditary Disease Foundation (HDF). N.P. is an Investigator of the Howard Hughes Medical Institute.

COMPETING INTERESTS

The authors declare no competing financial interests.

AUTHOR CONTRIBUTIONS

S.Z., M.B.F., J.T.L. and N.P. conceived the experiments; S.Z. performed and analyzed most of the experiments with the exception of the electrophysiological studies reported in Fig. 6, which were executed and interpreted by S.S. and J.T.L.; M.B.F. performed histology analyses and assessment of *dhtt-ko* mutants and HD-Q93; *dhtt-ko* adults; S.Z. drafted most parts of the manuscript except for those reported in Fig. 6, which were prepared primarily by S.S. and J.T.L. All authors reviewed and discussed the manuscript.

SUPPLEMENTARY MATERIAL

Supplementary material for this article is available at
http://dmm.biologists.org/lookup/suppl/doi:10.1242/dmm.000653/-/DC1

Received 21 April 2008; Accepted 14 January 2009.

REFERENCES

Andrade, M. A. and Bork, P. (1995). HEAT repeats in the Huntington's disease protein. *Nat. Genet.* **11**, 115-116.

Andrade, M. A., Petosa, C., O'Donoghue, S. I., Muller, C. W. and Bork, P. (2001). Comparison of ARM and HEAT protein repeats. *J. Mol. Biol.* **309**, 1-18.

Atkinson, N. S., Robertson, G. A. and Ganetzky, B. (1991). A component of calcium-activated potassium channels encoded by the Drosophila slo locus. *Science* **253**, 551-555.

Auerbach, W., Hurlbert, M. S., Hilditch-Maguire, P., Wadghiri, Y. Z., Wheeler, V. C., Cohen, S. I., Joyner, A. L., MacDonald, M. E. and Turnbull, D. H. (2001). The HD mutation causes progressive lethal neurological disease in mice expressing reduced levels of huntingtin. *Hum. Mol. Genet.* **10**, 2515-2523.

Budnik, V. and Gramates, L. S. (1999). *Neuromuscular Junctions in Drosophila*. San Diego, CA: London: Academic Press.

Budnik, V., Koh, Y. H., Guan, B., Hartmann, B., Hough, C., Woods, D. and Gorczyca, M. (1996). Regulation of synapse structure and function by the Drosophila tumor suppressor gene dlg. *Neuron* **17**, 627-640.

Cattaneo, E., Rigamonti, D., Goffredo, D., Zuccato, C., Squitieri, F. and Sipione, S. (2001). Loss of normal huntingtin function: new developments in Huntington's disease research. *Trends Neurosci.* **24**, 182-188.

Cattaneo, E., Zuccato, C. and Tartari, M. (2005). Normal huntingtin function: an alternative approach to Huntington's disease. *Nat. Rev. Neurosci.* **6**, 919-930.

Chopra, V. S., Metzler, M., Rasper, D. M., Engqvist-Goldstein, A. E., Singaraja, R., Gan, L., Fichter, K. M., McCutcheon, K., Drubin, D., Nicholson, D. W. et al. (2000). HIP12 is a non-proapoptotic member of a gene family including HIP1, an interacting protein with huntingtin. *Mamm. Genome* **11**, 1006-1015.

Clark, I. E., Dodson, M. W., Jiang, C., Cao, J. H., Huh, J. R., Seol, J. H., Yoo, S. J., Hay, B. A. and Guo, M. (2006). Drosophila pink1 is required for mitochondrial function and interacts genetically with parkin. *Nature* **441**, 1162-1166.

Coyle, I. P., Koh, Y. H., Lee, W. C., Slind, J., Fergestad, T., Littleton, J. T. and Ganetzky, B. (2004). Nervous wreck, an SH3 adaptor protein that interacts with Wsp, regulates synaptic growth in Drosophila. *Neuron* **41**, 521-534.

Dean, M., Rzhetsky, A. and Allikmets, R. (2001). The human ATP-binding cassette (ABC) transporter superfamily. *Genome Res.* **11**, 1156-1166.

DiFiglia, M., Sapp, E., Chase, K., Schwarz, C., Meloni, A., Young, C., Martin, E., Vonsattel, J. P., Carraway, R., Reeves, S. A. et al. (1995). Huntingtin is a cytoplasmic protein associated with vesicles in human and rat brain neurons. *Neuron* **14**, 1075-1081.

Dragatsis, I., Efstratiadis, A. and Zeitlin, S. (1998). Mouse mutant embryos lacking huntingtin are rescued from lethality by wild-type extraembryonic tissues. *Development* **125**, 1529-1539.

Dragatsis, I., Levine, M. S. and Zeitlin, S. (2000). Inactivation of Hdh in the brain and testis results in progressive neurodegeneration and sterility in mice. *Nat. Genet.* **26**, 300-306.

Duyao, M. P., Auerbach, A. B., Ryan, A., Persichetti, F., Barnes, G. T., McNeil, S. M., Ge, P., Vonsattel, J. P., Gusella, J. F., Joyner, A. L. et al. (1995). Inactivation of the mouse Huntington's disease gene homolog Hdh. *Science* **269**, 407-410.

Eaton, B. A., Fetter, R. D. and Davis, G. W. (2002). Dynactin is necessary for synapse stabilization. *Neuron* **34**, 729-741.

Engelender, S., Sharp, A. H., Colomer, V., Tokito, M. K., Lanahan, A., Worley, P., Holzbaur, E. L. and Ross, C. A. (1997). Huntingtin-associated protein 1 (HAP1) interacts with the p150Glued subunit of dynactin. *Hum. Mol. Genet.* **6**, 2205-2212.

Farah, M. H. (2007). RNAi silencing in mouse models of neurodegenerative diseases. *Curr. Drug Deliv.* **4**, 161-167.

Feany, M. B. and Bender, W. W. (2000). A Drosophila model of Parkinson's disease. *Nature* **404**, 394-398.

Ganetzky, B. and Flanagan, J. R. (1978). On the relationship between senescence and age-related changes in two wild-type strains of Drosophila melanogaster. *Exp. Gerontol.* **13**, 189-196.

Gindhart, J. G., Jr, Desai, C. J., Beushausen, S., Zinn, K. and Goldstein, L. S. (1998). Kinesin light chains are essential for axonal transport in Drosophila. *J. Cell Biol.* **141**, 443-454.

Greene, J. C., Whitworth, A. J., Kuo, I., Andrews, L. A., Feany, M. B. and Pallanck, L. J. (2003). Mitochondrial pathology and apoptotic muscle degeneration in Drosophila parkin mutants. *Proc. Natl. Acad. Sci. USA* **100**, 4078-4083.

Guan, Z., Saraswati, S., Adolfsen, B. and Littleton, J. T. (2005). Genome-wide transcriptional changes associated with enhanced activity in the Drosophila nervous system. *Neuron* **48**, 91-107.

Gunawardena, S. and Goldstein, L. S. (2001). Disruption of axonal transport and neuronal viability by amyloid precursor protein mutations in Drosophila. *Neuron* **32**, 389-401.

Gunawardena, S., Her, L. S., Brusch, R. G., Laymon, R. A., Niesman, I. R., Gordesky-Gold, B., Sintasath, L., Bonini, N. M. and Goldstein, L. S. (2003). Disruption of axonal transport by loss of huntingtin or expression of pathogenic polyQ proteins in Drosophila. *Neuron* **40**, 25-40.

Gusella, J. F. and MacDonald, M. E. (1995). Huntington's disease. *Semin. Cell Biol.* **6**, 21-28.

Gusella, J. F. and MacDonald, M. E. (2000). Molecular genetics: unmasking polyglutamine triggers in neurodegenerative disease. *Nat. Rev. Neurosci.* **1**, 109-115.

Gutekunst, C. A., Levey, A. I., Heilman, C. J., Whaley, W. L., Yi, H., Nash, N. R., Rees, H. D., Madden, J. J. and Hersch, S. M. (1995). Identification and localization of huntingtin in brain and human lymphoblastoid cell lines with anti-fusion protein antibodies. *Proc. Natl. Acad. Sci. USA* **92**, 8710-8714.

Harjes, P. and Wanker, E. E. (2003). The hunt for huntingtin function: interaction partners tell many different stories. *Trends Biochem. Sci.* **28**, 425-433.

Hauptmann, G. and Gerster, T. (2000). Multicolor whole-mount in situ hybridization. *Methods Mol. Biol.* **137**, 139-148.

Higgins, M. K. and McMahon, H. T. (2002). Snap-shots of clathrin-mediated endocytosis. *Trends Biochem. Sci.* **27**, 257-263.

Hinshaw, J. E. (2000). Dynamin and its role in membrane fission. *Annu. Rev. Cell Dev. Biol.* **16**, 483-519.

Holbert, S., Dedeoglu, A., Humbert, S., Saudou, F., Ferrante, R. J. and Neri, C. (2003). Cdc42-interacting protein 4 binds to huntingtin: neuropathologic and biological evidence for a role in Huntington's disease. *Proc. Natl. Acad. Sci. USA* **100**, 2712-2717.

Huang, C. C., Faber, P. W., Persichetti, F., Mittal, V., Vonsattel, J. P., MacDonald, M. E. and Gusella, J. F. (1998). Amyloid formation by mutant huntingtin: threshold, progressivity and recruitment of normal polyglutamine proteins. *Somat. Cell Mol. Genet.* **24**, 217-233.

Hummel, T., Krukkert, K., Roos, J., Davis, G. and Klambt, C. (2000). Drosophila Futsch/22C10 is a MAP1B-like protein required for dendritic and axonal development. *Neuron* **26**, 357-370.

Joiner, M. A. and Griffith, L. C. (1999). Mapping of the anatomical circuit of CaM kinase-dependent courtship conditioning in Drosophila. *Learn. Mem.* **6**, 177-192.

Kalchman, M. A., Koide, H. B., McCutcheon, K., Graham, R. K., Nichol, K., Nishiyama, K., Kazemi-Esfarjani, P., Lynn, F. C., Wellington, C., Metzler, M. et al. (1997). HIP1, a human homologue of S. cerevisiae Sla2p, interacts with membrane-associated huntingtin in the brain. *Nat. Genet.* **16**, 44-53.

Kazantsev, A., Preisinger, E., Dranovsky, A., Goldgaber, D. and Housman, D. (1999). Insoluble detergent-resistant aggregates form between pathological and nonpathological lengths of polyglutamine in mammalian cells. *Proc. Natl. Acad. Sci. USA* **96**, 11404-11409.

Koh, Y. H., Popova, E., Thomas, U., Griffith, L. C. and Budnik, V. (1999). Regulation of DLG localization at synapses by CaMKII-dependent phosphorylation. *Cell* **98**, 353-363.

Kulkarni, M. M., Booker, M., Silver, S. J., Friedman, A., Hong, P., Perrimon, N. and Mathey-Prevot, B. (2006). Evidence of off-target effects associated with long dsRNAs in Drosophila melanogaster cell-based assays. *Nat. Methods* **3**, 833-838.

Le Bourg, E. and Lints, F. A. (1992). Hypergravity and aging in Drosophila melanogaster. 4. Climbing activity. *Gerontology* **38**, 59-64.

Leavitt, B. R., Guttman, J. A., Hodgson, J. G., Kimel, G. H., Singaraja, R., Vogl, A. W. and Hayden, M. R. (2001). Wild-type huntingtin reduces the cellular toxicity of mutant huntingtin *in vivo*. *Am. J. Hum. Genet.* **68**, 313-324.

Li, Z., Karlovich, C. A., Fish, M. P., Scott, M. P. and Myers, R. M. (1999). A putative Drosophila homolog of the Huntington's disease gene. *Hum. Mol. Genet.* **8**, 1807-1815.

Littleton, J. T., Bellen, H. J. and Perin, M. S. (1993). Expression of synaptotagmin in Drosophila reveals transport and localization of synaptic vesicles to the synapse. *Development* **118**, 1077-1088.

Liu, Y. F., Deth, R. C. and Devys, D. (1997). SH3 domain-dependent association of huntingtin with epidermal growth factor receptor signaling complexes. *J. Biol. Chem.* **272**, 8121-8124.

Lumsden, A. L., Henshall, T. L., Dayan, S., Lardelli, M. T. and Richards, R. I. (2007). Huntingtin-deficient zebrafish exhibit defects in iron utilization and development. *Hum. Mol. Genet.* **16**, 1905-1920.

Marsh, J. L. and Thompson, L. M. (2006). Drosophila in the study of neurodegenerative disease. *Neuron* **52**, 169-178.

Martin, J. B. and Gusella, J. F. (1986). Huntington's disease: pathogenesis and management. *N. Engl. J. Med.* **315**, 1267-1276.

Martin, M., Iyadurai, S. J., Gassman, A., Gindhart, J. G., Jr, Hays, T. S. and Saxton, W. M. (1999). Cytoplasmic dynein, the dynactin complex, and kinesin are interdependent and essential for fast axonal transport. *Mol. Biol. Cell* **10**, 3717-3728.

Modregger, J., DiProspero, N. A., Charles, V., Tagle, D. A. and Plomann, M. (2002). PACSIN 1 interacts with huntingtin and is absent from synaptic varicosities in presymptomatic Huntington's disease brains. *Hum. Mol. Genet.* **11**, 2547-2558.

Narain, Y., Wyttenbach, A., Rankin, J., Furlong, R. A. and Rubinsztein, D. C. (1999). A molecular investigation of true dominance in Huntington's disease. *J. Med. Genet.* **36**, 739-746.

Nasir, J., Floresco, S. B., O'Kusky, J. R., Diewert, V. M., Richman, J. M., Zeisler, J., Borowski, A., Marth, J. D., Phillips, A. G. and Hayden, M. R. (1995). Targeted disruption of the Huntington's disease gene results in embryonic lethality and behavioral and morphological changes in heterozygotes. *Cell* **81**, 811-823.

O'Kusky, J. R., Nasir, J., Cicchetti, F., Parent, A. and Hayden, M. R. (1999). Neuronal degeneration in the basal ganglia and loss of pallido-subthalamic synapses in mice with targeted disruption of the Huntington's disease gene. *Brain Res.* **818**, 468-479.

Park, J., Lee, S. B., Lee, S., Kim, Y., Song, S., Kim, S., Bae, E., Kim, J., Shong, M., Kim, J. M. et al. (2006). Mitochondrial dysfunction in Drosophila PINK1 mutants is complemented by parkin. *Nature* **441**, 1157-1161.

Parks, A. L., Cook, K. R., Belvin, M., Dompe, N. A., Fawcett, R., Huppert, K., Tan, L. R., Winter, C. G., Bogart, K. P., Deal, J. E. et al. (2004). Systematic generation of high-resolution deletion coverage of the Drosophila melanogaster genome. *Nat. Genet.* **36**, 288-292.

Phelan, P., Nakagawa, M., Wilkin, M. B., Moffat, K. G., O'Kane, C. J., Davies, J. A. and Bacon, J. P. (1996). Mutations in shaking-B prevent electrical synapse formation in the Drosophila giant fiber system. *J. Neurosci.* **16**, 1101-1113.

Preisinger, E., Jordan, B. M., Kazantsev, A. and Housman, D. (1999). Evidence for a recruitment and sequestration mechanism in Huntington's disease. *Philos. Trans. R. Soc. Lond. B Biol. Sci.* **354**, 1029-1034.

Rieckhof, G. E., Yoshihara, M., Guan, Z. and Littleton, J. T. (2003). Presynaptic N-type calcium channels regulate synaptic growth. *J. Biol. Chem.* **278**, 41099-41108.

Rigamonti, D., Bauer, J. H., De-Fraja, C., Conti, L., Sipione, S., Sciorati, C., Clementi, E., Hackam, A., Hayden, M. R., Li, Y. et al. (2000). Wild-type huntingtin protects from apoptosis upstream of caspase-3. *J. Neurosci.* **20**, 3705-3713.

Riley, B. E. and Orr, H. T. (2006). Polyglutamine neurodegenerative diseases and regulation of transcription: assembling the puzzle. *Genes Dev.* **20**, 2183-2192.

Roos, J., Hummel, T., Ng, N., Klambt, C. and Davis, G. W. (2000). Drosophila Futsch regulates synaptic microtubule organization and is necessary for synaptic growth. *Neuron* **26**, 371-382.

Seki, N., Muramatsu, M., Sugano, S., Suzuki, Y., Nakagawara, A., Ohhira, M., Hayashi, A., Hori, T. and Saito, T. (1998). Cloning, expression analysis, and chromosomal localization of HIP1R, an isolog of huntingtin interacting protein (HIP1). *J. Hum. Genet.* **43**, 268-271.

Sharp, A. H., Loev, S. J., Schilling, G., Li, S. H., Li, X. J., Bao, J., Wagster, M. V., Kotzuk, J. A., Steiner, J. P., Lo, A. et al. (1995). Widespread expression of Huntington's disease gene (IT15) protein product. *Neuron* **14**, 1065-1074.

Singaraja, R. R., Hadano, S., Metzler, M., Givan, S., Wellington, C. L., Warby, S., Yanai, A., Gutekunst, C. A., Leavitt, B. R., Yi, H. et al. (2002). HIP14, a novel ankyrin domain-containing protein, links huntingtin to intracellular trafficking and endocytosis. *Hum. Mol. Genet.* **11**, 2815-2828.

Sittler, A., Walter, S., Wedemeyer, N., Hasenbank, R., Scherzinger, E., Eickhoff, H., Bates, G. P., Lehrach, H. and Wanker, E. E. (1998). SH3GL3 associates with the Huntingtin exon 1 protein and promotes the formation of polygln-containing protein aggregates. *Mol. Cell* **2**, 427-436.

Slepnev, V. I. and De Camilli, P. (2000). Accessory factors in clathrin-dependent synaptic vesicle endocytosis. *Nat. Rev. Neurosci.* **1**, 161-172.

Steffan, J. S., Bodai, L., Pallos, J., Poelman, M., McCampbell, A., Apostol, B. L., Kazantsev, A., Schmidt, E., Zhu, Y. Z., Greenwald, M. et al. (2001). Histone deacetylase inhibitors arrest polyglutamine-dependent neurodegeneration in Drosophila. *Nature* **413**, 739-743.

Sullivan, W., Ashburner, M. and Hawley, R. S. (2000). *Drosophila Protocols*. Cold Spring Harbor, NY: Cold Spring Harbor Laboratory Press.

Sun, Y., Savanenin, A., Reddy, P. H. and Liu, Y. F. (2001). Polyglutamine-expanded huntingtin promotes sensitization of N-methyl-D-aspartate receptors via post-synaptic density 95. *J. Biol. Chem.* **276**, 24713-24718.

Tartari, M., Gissi, C., Lo Sardo, V., Zuccato, C., Picardi, E., Pesole, G. and Cattaneo, E. (2008). Phylogenetic comparison of huntingtin homologues reveals the appearance of a primitive polyQ in sea urchin. *Mol. Biol. Evol.* **25**, 330-338.

The Huntington's Disease Collaborative Research Group (1993). A novel gene containing a trinucleotide repeat that is expanded and unstable on Huntington's disease chromosomes. *Cell* **72**, 971-983.

Van Raamsdonk, J. M., Pearson, J., Rogers, D. A., Bissada, N., Vogl, A. W., Hayden, M. R. and Leavitt, B. R. (2005). Loss of wild-type huntingtin influences motor dysfunction and survival in the YAC128 mouse model of Huntington disease. *Hum. Mol. Genet.* **14**, 1379-1392.

Vonsattel, J. P. and DiFiglia, M. (1998). Huntington disease. *J. Neuropathol. Exp. Neurol.* **57**, 369-384.

Vonsattel, J. P., Myers, R. H., Stevens, T. J., Ferrante, R. J., Bird, E. D. and Richardson, E. P., Jr (1985). Neuropathological classification of Huntington's disease. *J. Neuropathol. Exp. Neurol.* **44**, 559-577.

Wang, P., Saraswati, S., Guan, Z., Watkins, C. J., Wurtman, R. J. and Littleton, J. T. (2004). A Drosophila temperature-sensitive seizure mutant in phosphoglycerate kinase disrupts ATP generation and alters synaptic function. *J. Neurosci.* **24**, 4518-4529.

Wanker, E. E., Rovira, C., Scherzinger, E., Hasenbank, R., Walter, S., Tait, D., Colicelli, J. and Lehrach, H. (1997). HIP-I: a huntingtin interacting protein isolated by the yeast two-hybrid system. *Hum. Mol. Genet.* **6**, 487-495.

Wheeler, V. C., White, J. K., Gutekunst, C. A., Vrbanac, V., Weaver, M., Li, X. J., Li, S. H., Yi, H., Vonsattel, J. P., Gusella, J. F. et al. (2000). Long glutamine tracts cause nuclear localization of a novel form of huntingtin in medium spiny striatal neurons in HdhQ92 and HdhQ111 knock-in mice. *Hum. Mol. Genet.* **9**, 503-513.

White, J. K., Auerbach, W., Duyao, M. P., Vonsattel, J. P., Gusella, J. F., Joyner, A. L. and MacDonald, M. E. (1997). Huntingtin is required for neurogenesis and is not impaired by the Huntington's disease CAG expansion. *Nat. Genet.* **17**, 404-410.

Zeitlin, S., Liu, J. P., Chapman, D. L., Papaioannou, V. E. and Efstratiadis, A. (1995). Increased apoptosis and early embryonic lethality in mice nullizygous for the Huntington's disease gene homologue. *Nat. Genet.* **11**, 155-163.

Zoghbi, H. Y. and Orr, H. T. (2000). Glutamine repeats and neurodegeneration. *Annu. Rev. Neurosci.* **23**, 217-247.

Zuccato, C. and Cattaneo, E. (2007). Role of brain-derived neurotrophic factor in Huntington's disease. *Prog. Neurobiol.* **81**, 294-330.

Zuccato, C., Ciammola, A., Rigamonti, D., Leavitt, B. R., Goffredo, D., Conti, L., MacDonald, M. E., Friedlander, R. M., Silani, V., Hayden, M. R. et al. (2001). Loss of huntingtin-mediated BDNF gene transcription in Huntington's disease. *Science* **293**, 493-498.

Zuccato, C., Belyaev, N., Conforti, P., Ooi, L., Tartari, M., Papadimou, E., MacDonald, M., Fossale, E., Zeitlin, S., Buckley, N. et al. (2007). Widespread disruption of repressor element-1 silencing transcription factor/neuron-restrictive silencer factor occupancy at its target genes in Huntington's disease. *J. Neurosci.* **27**, 6972-6983.